PROCEEDINGS OF SCIENCE

Neutrino Physics

Pablo Martínez-Miravé,[a] **Kristjan Müürsepp**[b] **and Mariam Tórtola**[a,*]

[a] *Departament de Física Teòrica, Universitat de València, and Instituto de Física Corpuscular, CSIC-Universitat de València, 46980 Paterna, Spain*

[b] *National Institute of Chemical Physics and Biophysics, Rävala 10, 10143 Tallinn, Estonia*

E-mail: kristjan.muursepp@kbfi.ee, pablo.m.mirave@ific.uv.es, mariam@ific.uv.es

These lectures provide a general overview of the current status of neutrino physics with an emphasis in the phenomenology of neutrino oscillations and the searches for physics beyond the Standard Model.

Corfu Summer Institute 2021 "School and Workshops on Elementary Particle Physics and Gravity"
29 August - 9 October 2021
Corfu, Greece

*Speaker

© Copyright owned by the author(s) under the terms of the Creative Commons Attribution-NonCommercial-NoDerivatives 4.0 International License (CC BY-NC-ND 4.0).

PoS(CORFU2021)321

1. Introduction

For decades, the Standard Model (SM) of particle physics has provided a great understanding of the behaviour of elementary particles and their interactions. However, albeit successful in describing a plethora of elementary processes, it is clear from several observational facts that the SM cannot be the ultimate theory of particle physics. The first and more solid evidence so far is the observation of nonzero neutrino masses, which can not be accommodated within the SM. Thus, neutrino physics offers an important pathway to exploring different options to beyond the SM physics, while also having important connections to different phenomena in cosmology and astrophysics.

Neutrinos are elementary spin one-half particles, with no electric charge. Similarly to the quarks and the charged leptons, neutrinos come in three different flavours or families. Although initially considered massless, neutrinos actually do have a nonzero, albeit very small mass in comparison to other observed elementary particles.

Despite being very difficult to observe, neutrinos are in fact all around us. Every second, we are traversed by several hundred billions (10^{12}) of neutrinos arriving from the Sun and thousands of millions of neutrinos produced by Earth's radioactivity and by nuclear power plants. In addition to being immersed in such enormous flux of neutrinos, our body also emits 400 neutrinos per second through the radioactive decay of ^{40}K. On a larger scale, the Universe is permeated by the cosmic neutrino background, a relic of the Big Bang, consisting of ~ 300 neutrinos per cubic centimeter.

The abundance of neutrinos, however, is not the main reason to study these elusive particles. Actually, neutrino physics offers an indirect probe to otherwise observationally inaccessible phenomena such as supernova explosions or nuclear processes in the core of the Sun. On a cosmological scale, neutrinos can be used to study the evolution of the Universe through their imprint on Big Bang nucleosynthesis and structure formation. Moreover, in the realm of particle physics, neutrinos could also be the key ingredient to solving the matter-antimatter problem via the leptogenesis mechanism or provide a viable candidate to (part of the) dark matter. Finally, as already commented, the observation of non-zero neutrino masses provides the first evidence for the existence of physics beyond the SM.

These lecture notes on neutrino physics are organized as follows. After a short introduction, Section 2 provides a summary of the historical development of neutrino physics. In Section 3, neutrino interactions and masses in the context of the Standard Model are discussed. Next, Section 4 addresses the issue of the neutrino mass models beyond the Standard Model, discussing also the difference between Majorana and Dirac particles and presenting the current experimental constraints on the absolute mass scale. Section 5 outlines the basics of neutrino oscillations, summarizing the historical context as well as the formalism of neutrino oscillations in vacuum and in matter. In Section 6, the experimental results from neutrino oscillations are presented, including a discussion on the existing data and the current status of the determination of the parameters describing the phenomenon. The experimental status of searches for additional light (sterile) neutrinos is addressed in Section 7, whereas other Beyond the Standard Model scenarios which impact the neutrino sector, such as non-standard interactions, non-unitarity of the 3 neutrino mixing matrix and CPT and Lorentz invariance violation, are covered in Section 8. Finally, Section 9 summarises the topics covered in these lecture notes.

PoS(CORFU2021)321

2. Historical introduction to neutrino physics

Here we summarize the most relevant facts that laid the foundations of neutrino physics. These include its postulation, the detection of the three neutrino flavors, and the discovery of parity violation in weak interactions, a fundamental key to understanding neutrino physics.

2.1 The discovery of neutrinos

The neutrino as an elementary particle was first proposed by Wolfgang Pauli in 1930 to explain the continuous energy spectrum of the electrons emitted at nuclear beta decays. Since their energy was not necessarily given by the difference of energies between the parent and daughter nuclei, the presence of another particle was needed to conserve energy. From the conservation of angular momentum, Pauli inferred that the spin of this new particle had to be $1/2$. This idea was then taken up by Enrico Fermi, who built the effective theory of weak interactions. This theory explained the neutron decay (and any nuclear beta decay) as resulting from its weak interaction with protons, electrons and antineutrinos, and controlled by a parameter G_F now known as the Fermi constant. Using the Fermi model, the beta decay can thus be schematically written as

$$n \to p + e^- + \overline{\nu}_e. \tag{1}$$

It was also Fermi who dubbed the new hypothetical particle the neutrino.
After the introduction of the Fermi theory of weak introductions, Hans Bethe and Rudolf Peierls used it to calculate the cross sections of processes involving neutrinos, such as:

$$\overline{\nu} + p \to n + e^+ . \tag{2}$$

Assuming an initial neutrino energy of 2 MeV, they obtained a cross section of $\sim 10^{-44} cm^2$ [1]. Comparing this result with the cross section of a typical electromagnetic process, $\sigma_{p\gamma} \approx 10^{-25} cm^2$, it was evident that neutrino interactions with matter were extremely weak. We can further emphasize this fact by estimating the mean free path of neutrinos in water and lead, whose values are $\lambda_w \approx 1.7 \times 10^{17} m = 15$ ly and $\lambda_l \approx 1.5 \times 10^{16} m = 1.5$ ly, respectively. This result naturally led to question whether detecting neutrinos was experimentally feasible at all. Actually, this is exactly what Pauli was worried about after his famous proposal in 1930, when he claimed [2]:

I have done a terrible thing, I have postulated a particle that cannot be detected.

Likewise, Bethe and Peierls concluded from their calculation that "there is no practically possible way of observing the neutrino" [1]. However, nowadays we know that neutrinos have been experimentally observed according to the predictions of the SM, meaning that there must be a way of overcoming the elusive nature of these particles. In order to understand how this can be done, we can perform a very simple estimate for the number of neutrino events (N) expected in a particular detector in a given amount of time Δt,

$$N = \phi \sigma n V \Delta t. \tag{3}$$

Here ϕ is the incoming flux of neutrinos, σ is the cross section of the interaction between the neutrinos and the target nuclei, n is the density of of the target nuclei per cubic meter and V is the

PoS(CORFU2021)321

volume of the detector. From Eq. (3), it can be seen that if the flux of the incoming neutrinos and the volume of the detector are large enough, it is definitely possible to detect some neutrino events in a reasonable timeframe. For example, for a flux of $\phi = 10^{10} \nu/(cm^2 s)$ and for a detector of mass $m = 1000\, kg$ a few events per day can be observed. A flux of this order of magnitude is definitely realistic given the flux of neutrinos from the sun, $\phi = 7 \times 10^{10} \nu/(cm^2 s)$ or from nuclear reactors, $\phi = 10^{20} \nu/(cm^2 s)$.

Indeed, it was precisely the large flux from the nuclear reactors that was used by Fred Reines and Clyde Cowan in 1956 to make the first detection of electron neutrinos. Although their initial plan was to install a detector underneath a nuclear bomb, this idea was abandoned as the necessary experimental setup was considered to be too unstable. Instead, 2 tanks of 200 litres of water and 40 kg of $CdCl_2$ were set up near the Savannah river reactor in the USA. The antineutrinos produced at the nuclear reactor interacted with protons from the water tanks producing neutrons and positrons through the inverse β-decay

$$\overline{\nu}_e + p \rightarrow n + e^+ \,. \tag{4}$$

The positrons then annihilated with the electrons from the detector producing two photons while the neutrons were absorbed by Cadmium, which emitted another photon after de-excitation. The photons were then observed by three scintillator layers with photomultiplier tubes. The coincident three-photon signal was then used to confirm that the antineutrino-proton interaction had happened. It is important to emphasize that using the three-photon coincidence signal was crucial to reduce the background events and finally confirm the existence of the, until then, hypothetical neutrinos [3]. The discovery of the electron neutrino at the Cowan-Reines experiment in 1956 received the Nobel Prize in Physics in 1995, awarded only to F. Reines since C. Cowan had passed away in 1974.

After the observation of the electron neutrino, Bruno Pontecorvo and, independently, Melvin Schwartz suggested in 1959 that perhaps there was also a second neutrino associated with the muon [4, 5], discovered at cosmic rays in 1936. In order to test this hypothesis, they proposed that muon neutrinos, presumably produced at particle accelerators, might be indirectly detected after interacting with neutrons according to the following process:

$$n + \nu_\mu \rightarrow p + \mu. \tag{5}$$

If such neutrinos were actually different from the ones discovered by Reines and Cowan, a muon, instead of an electron, would be detected in the final state.

This idea was put into practice in 1962 by Melvin Schwartz together with Leon Lederman and Jack Steinberger at Brookhaven National Laboratory, in the USA. They collided an accelerated proton beam into a target, producing π-mesons. These pions decayed into muons and muon neutrinos. The muons were stopped by a 13 m steel shield, while the muon neutrinos, due to their very weak interactions with matter, passed through it. Then, a very small fraction of the muon neutrinos interacted with the neutrons in the detector, producing protons and muons, as in Eq. (5). The detection of the resulting muons in a spark chamber led to the first detection of the muon neutrino [6], and Lederman, Schwartz and Steinberger won the Nobel prize in Physics in 1988 for this discovery.

PoS(CORFU2021)321

Later on, in 1978, imbalances in energy in the decay of the third generation lepton, the τ, suggested that there may also be a third generation neutrino, the tau neutrino, ν_τ. This belief was also enforced by the Z-boson invisible decay width measurements at LEP in 1988. In particular, using the invisible decay width, defined by

$$\Gamma_{\rm inv} = \Gamma_Z - \Gamma_{\rm had} - 3\Gamma_{\rm lep} \tag{6}$$

where Γ_Z denotes the total decay width of the Z boson, $\Gamma_{\rm had}$ the width of the Z decay into hadronic states and $\Gamma_{\rm lep}$ the decay of Z into the charged leptons. An estimate for the number of light neutrino generations was obtained as [7]

$$N_\nu = \frac{\Gamma_{\rm inv}}{\Gamma_{\rm SM}(Z \to \nu_i \bar{\nu}_i)} = 2.9840 \pm 0.0082. \tag{7}$$

The definitive confirmation of the existence of three generations of neutrinos in Nature arrived in 2000 when the Donut collaboration observed a tau-lepton in the decay of the D-meson resulting from a 800 GeV proton beam [8].

2.2 Parity violation in weak interactions

Going slightly back in time, there is another interesting phenomenon related to neutrinos that is worth addressing. In the 1950s, particle physicists were very confused by the so-called $\theta - \tau$ puzzle.These apparently distinct mesons had very similar properties but different decay channels:

$$\theta^+ \to \pi^+ + \pi^0 \tag{8}$$

$$\tau^+ \to \pi^+ + \pi^+ + \pi^-. \tag{9}$$

Since both of these mesons as well as the resulting pions were all pseudo-scalar particles, assuming parity conservation it seemed that θ would have even parity, while τ would be odd under parity. However, as stated before, all the other properties of these two particles were the same. Unwilling to accept this mysterious coincidence, in 1956, Tsung-Dao Lee and Chen-Ning Yang proposed that perhaps τ and θ were in fact the same particle and, consequently, parity would be manifestly violated in the decay of this meson [9]. To check their hypothesis, Chien-Shiung Wu designed an experiment in 1957 to check if actually parity was violated in the weak interactions. The experiment involved ^{60}Co nuclei cooled to a very low temperature, with their spins aligned to an external magnetic field. Since ^{60}Co nuclei are radioactively unstable, they quickly decayed through β-decay to ^{60}Ni followed by the electromagnetic emission of photons through the de-excitation of the resulting ^{60}Ni nuclei. The combined process of the radioactive decay and the emission of γ-rays can schematically be written as:

$$^{60}Co \;\to\; ^{60}Ni^* + e^- + \bar{\nu}_e \;\to\; ^{60}Ni + e^- + \bar{\nu}_e + 2\gamma\,. \tag{10}$$

The γ-rays were useful as a test probe since, as parity is conserved in the electromagnetic interactions, in ideal experimental conditions, they would be emitted isotropically. Consequently, these photons could be used to infer any anisotropy of the emitted electrons as well as to check how well the ^{60}Co nuclei were aligned with the magnetic field. As a result of the experiment, it was found that electrons were always emitted in a direction opposite to the spin of the nuclei, showing that parity is maximally violated in weak interactions [10]. A detailed look at the conservation

PoS(CORFU2021)321

of linear and angular momentum in the process in Eq. (10) indicates that the origin of parity violation lies in the fact that only antineutrinos emitted parallel to their spin (what we later will call *right-handed* antineutrinos) participate in weak interactions. As a consequence of this experimental result, Lee and Yang were awarded the Nobel prize in Physics in 1957 for their proposal of the violation of parity in the weak interactions and Wu received the first Wolf prize in 1978. Later on, in 1958, the experiment conducted by Goldhaber and collaborators further confirmed that indeed only *left-handed* neutrinos (and *right-handed* antineutrinos) participate in the weak interactions [11].

In the previous paragraphs we have mentioned the idea of right and left-handed particles. In order to be more clear about this, it is necessary to understand the terms *helicity* and *chirality*. The *helicity* operator $\hat{H}$ for a particle is defined by the projection of the particles' spin to its momentum

$$\hat{H} = \frac{\vec{s}\cdot\vec{p}}{|\vec{s}\cdot\vec{p}|} = \pm 1\,. \tag{11}$$

Helicity can be directly measured in an experiment, as discussed above concerning the Wu experiment. However, it is a Lorentz invariant quantity only for massless particles, since for a massive particle it is always possible to boost to a new frame where the particle has an opposite momentum and thus opposite helicity. For a massless particle, this is not possible since in that case the particle already moves at the maximum possible speed, the speed of light. The *chirality* of a fermion field is a Lorentz-invariant quantity related to behaviour of the field under Lorentz transformations. It can be thought of as an asymmetry property, since chiral objects are not identical to their mirror image. The chiral components of the fermion field ψ, ψ_L and ψ_R, can be projected out by using the projection operator

$$P_{L,R} = \frac{1 \mp \gamma_5}{2} \quad \rightarrow \quad \psi_{L,R} = P_{L,R}\psi\,. \tag{12}$$

Chirality is not a directly measurable quantity and, therefore, it can be useful to relate it to helicity, which can actually be measured. However, one should be careful with the relation between the two magnitudes, since they are exactly equivalent only for massless particles. In general, for massive particles, a chiral state contains a mixture of the two (positive and negative) helicity states. An intermediate scenario is realized by ultrarelativistic particles, since in this case the left-handed chiral projection is dominated by the negative helicity state and the right-handed chiral projection is dominated by the positive helicity state. This is why for neutrinos, that have only a very small mass, one can talk about the observation of left and right handed neutrinos (at Wu or Goldhaber experiments) even though what is actually measured is the helicity.

3. Neutrinos in the Standard Model

The Standard Model of particle physics is a gauge field theory based on the symmetry group $SU(3)_C \times SU(2)_L \times U(1)_Y$, where C stands for color, L for left-handedness and Y for hypercharge. Thus, neutrinos are part, together with the associated charged leptons, of the lepton doublets

$$L_{L\alpha} = \begin{pmatrix} \nu_\alpha \\ l^-_\alpha \end{pmatrix}_L\,. \tag{13}$$

Here, L refers to the left-handed component of the field, $\psi_L = P_L\psi$, and α denotes the flavor of the lepton doublet, $\alpha = e, \mu, \tau$

PoS(CORFU2021)321

3.1 Neutrino interactions in the Standard Model

In the SM, neutrinos can interact with their corresponding charged leptons through the weak charged current (CC) interaction and among themselves through the weak neutral current (NC) interaction. The former one can be written down using the following Lagrangian,

$$\mathcal{L}_{CC} = -\frac{g}{\sqrt{2}} \sum_{\alpha} \bar{\nu}_{\alpha} \gamma^{\mu} l_{\alpha L} W_{\mu} + h.c. \tag{14}$$

where, as before, α denotes the different families of neutrinos and the associated charged leptons, $\alpha = e, \mu, \tau$. Thus, neutrinos and charged leptons can be produced by the decay of the W boson as follows

$$W^- \to l^-_{\alpha} + \bar{\nu}_{\alpha} \tag{15}$$

$$W^+ \to l^+_{\alpha} + \nu_{\alpha} \,. \tag{16}$$

Notice that the discoveries of the three neutrino species described in the previous section took place through CC weak interaction processes, involving neutrinos and charged leptons.

The NC interaction, instead, involves only neutrinos and it is mediated by the Z boson. The corresponding lagrangian is given by

$$\mathcal{L}_{NC} = -\frac{g}{2\cos\theta_W} \sum_{\alpha} \bar{\nu}_{\alpha L} \gamma^{\mu} \nu_{\alpha L} Z^0_{\mu} \,. \tag{17}$$

where g (appearing in Eq. (14) too) is the coupling constant associated to $SU(2)$ and θ_W is the electroweak mixing angle, also known as Weinberg angle. Neutrinos can then also be produced by the decay of the Z boson as follows:

$$Z^0 \to \nu_{\alpha} \bar{\nu}_{\alpha} \,. \tag{18}$$

Note that the existence of weak neutral currents, predicted in the mid 1960s by the consistency of the electroweak theory [12, 13], was not confirmed until 1973 when a process of the type $\nu_{\mu} + N \to \nu_{\mu} +$ hadrons was first observed at the CERN Gargamelle bubble chamber [14].

These interactions conserve the total lepton number, L, defined as

$$L(l^-) = L(\nu) = -L(l^+) = -L(\bar{\nu}) = 1 \,. \tag{19}$$

For a long time it was thought that the individual lepton family numbers L_e, L_{μ} and L_{τ} were also conserved, but this assumption was refuted by the discovery of neutrino oscillations in 1998.

3.2 Neutrino masses in the Standard Model

In the context of the SM, fermion masses are introduced in the Lagrangian with terms of the form $m\bar{\psi}\psi$. Decomposing the fields into their chiral (left-handed and right-handed) states, $\psi = \psi_L + \psi_R$, and considering the definition of the projector operators in Eq. (12), one has

$$m\bar{\psi}\psi = m(\overline{\psi}_L + \overline{\psi}_R)(\psi_L + \psi_R) = m\overline{\psi}_L\psi_R + m\overline{\psi}_R\psi_L \,. \tag{20}$$

Hence, the mass term for fermions involves both left and right-handed chiral states. However, in the SM the former transform as doublets under $SU(2)_L$, while the latter are singlets under this group.

PoS(CORFU2021)321

In consequence, the mass term as given above one cannot be directly written down , since it would break gauge invariance. Instead, one has to consider the Higgs mechanism, whereby the coupling between the fermions and a scalar ϕ, the Higgs doublet is introduced

$$\mathcal{L}_{\text{Yukawa}} = Y\overline{\psi}_L \phi \psi_R + h.c. \tag{21}$$

Then, after the neutral component of the Higgs doublet is assigned a non-zero vacuum expectation value, the $SU(2)_L$ symmetry is spontaneously broken, generating a mass term for the fermions. And this is how the Higgs mechanism accounts for the masses of all fermions in the SM with the exception of neutrinos. The reason why the Higgs mechanism cannot be used to accommodate neutrino masses within the SM is simply because it does not contain right-handed neutrino fields, a necessary ingredient to build the mass term in Eq. (21). Consequently, neutrinos are strictly massless in the SM and therefore new physics beyond the SM needs to be sought to explain neutrino masses.

4. Neutrino masses beyond the Standard Model

As we will see in the next section, the existence of neutrino oscillations imply that neutrinos are massive. Here we will summarize some extensions of the SM providing possible explanations for the origin of neutrino masses. This will also include a brief discussion on the Dirac or Majorana nature of neutrinos, a key issue in the construction of neutrino mass models.

4.1 The nature of neutrinos: Dirac or Majorana?

From the previous discussion, we can see that, in order to describe the observed non-zero neutrino masses, one needs to introduce new chiral states, namely a right-handed state for the neutrino and a left-handed state for the antineutrino, since the SM only contains left-handed states for the former and right-handed states for the latter. Here we should point out that the neutrino case may be qualitatively different from the charged lepton case. In effect, although in the case of charged leptons there is no possible connection between the chiral states of a particle and its antiparticle, the null electric charge of neutrinos allows the identification of neutrino and antineutrino chiral states. Let us explain this point in more detail. As mentioned before, for massive particles, it is always possible to perform a Lorentz boost to a frame in which the left-handed state becomes the right handed state [1]. Nevertheless, since the Lorentz boost cannot flip the electric charge of a particle, applying the boost to a left-handed electron estate e_L will result in a right-handed electron state e_R but never in a positron right-handed state $\overline{e_L}$. In the case of neutrinos, however, the two possibilities can occur. In the first case, the left-handed neutrino state ν_L will result in a (new) right-handed neutrino state N_R but, in addition, it would also be possible identifying the boosted state with the existing right-handed antineutrino state $\overline{\nu_L}$. In other words, a neutrino can also be its own antiparticle. These two options essentially define the Dirac (first case) and Majorana (second option) nature of neutrinos, which has profound implications for the building of neutrino mass terms.

[1] One should note that for the massive case the left and right-handed chirality states do not exactly coincide with the helicity states but, given that this difference is suppressed for very light particles, we can still talk about the handedness of the helicity eigenstates.

PoS(CORFU2021)321

In the Dirac case, one can extend the SM with the new field N_R and thus write down the mass term as

$$-\mathcal{L}_D = m_D \left(\overline{\nu_L} N_R + \overline{N_R} \nu_L\right). \tag{22}$$

This term is invariant under a U(1) transformation, and therefore the electric charge and the baryon and lepton number are all conserved in the theory.

The second possibility is to use Majorana fermions. In that case, the new neutrino chiral state ν_R is obtained from the SM field as

$$\nu_R \equiv \nu_L^C = \hat{C}\bar{\nu}^T, \qquad \hat{C} = i\gamma^2\gamma^0. \tag{23}$$

The fermion field can then be decomposed as

$$\nu = \nu_L + \nu_L^C. \tag{24}$$

And therefore

$$\nu^C = (\nu_L + \nu_R)^C = \nu_L^C + \nu_L = \nu \tag{25}$$

what explains why it is often said that a Majorana neutrino is its own antiparticle. The Majorana mass term is then built as

$$-\mathcal{L}_M = \frac{1}{2} m \left(\overline{\nu_L^C} \nu_L + \overline{\nu_L} \nu_L^C\right) \tag{26}$$

Unlike the Dirac mass term, note that this mass term is not invariant under U(1) transformations. Hence, Majorana mass for neutrinos breaks the lepton number by two units. Moreover, this mass term is not $SU(2)_L$ invariant either, and then it cannot be directly added to the SM Lagrangian. One option to generate this term is given by the dimension-5 Weinberg operator [15] which is, however, non-renormalizable and will not be covered in these lectures. Other possible extensions of the SM allowing for non-zero neutrino masses will be discussed below.

4.2 Neutrino mass models

If one wishes to generate the neutrino masses in the same way as for the other fermions in the SM, it is possible to add a new field N_R to the SM, usually called the "sterile neutrino field". The reason for calling it "sterile" is that N_R is a singlet under the SM gauge group $SU(3)_C \times SU(2)_L \times U(1)_Y$. In that case, a Dirac mass term appears in the Lagrangian in the following way:

$$-\mathcal{L}_D = m_D \bar{\nu}\nu = m_D \left(\overline{\nu_L} + \overline{N_R}\right)(\nu_L + N_R) = m_D \left(\overline{\nu_L} N_R + \overline{N_R} \nu_L\right). \tag{27}$$

In order to get an estimate for the size of the neutrino mass m_D that should be then generated by spontaneous symmetry breaking, we note that from neutrino oscillation data one has

$$m_\nu \geq \sqrt{\Delta m^2_{31}} = 0.05\,\text{eV}. \tag{28}$$

For the SM-like Higgs mechanism scenario, we can write down the Yukawa coupling

$$\mathcal{L}_{\text{Yukawa}} = Y_\nu \left(\overline{\nu_\alpha} \quad \overline{l_\alpha}\right) \begin{pmatrix} \phi^0 \\ \phi^- \end{pmatrix} N_R + \text{h.c.} \tag{29}$$

PoS(CORFU2021)321

Then, after the electroweak symmetry is spontaneously broken and the Higgs field gets a non-zero vacuum expectation value, we have that

$$\langle \phi \rangle = \frac{1}{\sqrt{2}} \begin{pmatrix} v \\ 0 \end{pmatrix} \quad \rightarrow \quad m_\nu = Y_\nu \frac{v}{\sqrt{2}} \,. \tag{30}$$

Then, to reproduce the observed order of magnitude of neutrino masses, the Yukawa coupling Y_ν should be of the order of 10^{-13}. Compared to the Yukawa coupling for the charged leptons that are in the same doublet as the neutrinos (e.g for electron $Y_e \simeq 10^{-5}$), we note that the Yukawa coupling for the neutrino should be at least 8 orders of magnitude smaller than for the electron. This huge hierarchy between the dimensionless couplings for two fermions in the same doublet indicates a high degree of fine tuning and hence it is undesired on naturalness grounds. Hence, alternative mechanisms responsible for the nonzero neutrino masses are called for.

This issue is naturally addressed by the *seesaw mechanism*, the most popular class of models among the different neutrino mass generation models. The seesaw mechanism uses two different Majorana fermions $\nu = \nu_L + \nu_L^C$, where ν_L is a $SU(2)_L$ doublet and $N = N_R + N_R^C$, where N_R is a SM singlet. With these ingredients, the general mass term in the Lagrangian can be written as

$$\mathcal{L} = \mathcal{L}_D + \mathcal{L}_M = \frac{1}{2} \begin{pmatrix} \overline{\nu_L} & \overline{N_R^C} \end{pmatrix} \begin{pmatrix} 0 & m_D \\ m_D & M_R \end{pmatrix} \begin{pmatrix} \nu_L^C \\ N_R \end{pmatrix} + \text{h.c.} \tag{31}$$

Note that the Majorana mass term for N_R, M_R, can be written since it is a $SU(2)_L$ singlet, while for the $SU(2)_L$ doublet ν_L the Majorana mass term cannot be added due to gauge invariance. The mass matrix given above can be easily diagonalized by a unitary transformation, after which one obtains two different mass eigenstates M_1 and M_2 corresponding to the physical neutrino masses. If $M_R >> m_D$, the mass eigenstates can be approximated by

$$M_1 \simeq \frac{m_D^2}{M_R} \,, \quad M_2 \simeq M_R \,. \tag{32}$$

It then follows immediately that $M_1 << M_2$ since M_1 is suppressed by the heavy mass scale M_R. If one chooses $M_R \simeq 10^{14}$ TeV, SM neutrino masses of the order 1 eV can be generated while the heavy neutrino mass scale is much above the limit of our current experimental capabilities. Note also that since the seesaw models necessarily make use of Majorana leptons that violate the lepton number by two units, one can use these models to also explain the baryon asymmetry of the universe through the leptogenesis mechanism [16]. In particular, one could use the CP violation in the decay of the heavy sterile neutrino

$$\Gamma(N \rightarrow l + H) \neq \Gamma(N \rightarrow \bar{l} + \overline{H}) \,. \tag{33}$$

to explain the matter-antimatter asymmetry.

The seesaw model used above is the simplest example of the many possible ways of constructing such models. It is usually called Type-I seesaw model. For that scenario, if one takes into account all three generations of neutrinos the neutrino mass term can be written as [17–20]

$$m_\nu = Y_N^T \frac{1}{M_N} Y_N \, v^2 \,. \tag{34}$$

PoS(CORFU2021)321

In a slightly more complicated realization of the seesaw model (known as Type-II), it is also possible to replace the singlet N_R with a scalar triplet Δ. In that case, the resulting mass matrix is given by [21–25]

$$m_\nu = Y_\Delta \frac{\mu_\Delta}{M_\Delta^2} v^2 \,. \tag{35}$$

Finally, instead of using scalar triplet, one can also use a fermion triplet. In this case, the model is known as seesaw Type-III and the mass matrix can be written as [26]

$$m_\nu = Y_\Sigma^T \frac{1}{M_\Sigma} Y_\Sigma v^2 \,. \tag{36}$$

Note that in each of these cases (seesaw Type-I, II and III) the light neutrino masses originate from the suppression of the mass of the heavy mediator. Crucially, all of these models require a mediator with mass that is certainly outside the reach of current experiments.

To find a more testable model, one could consider a slightly different construction, known as the *inverse seesaw model*. In that case, one introduces two $SU(2)_L$ singlet Majorana fermions N_R and S. The mass matrix that is then generated is given by [27]

$$M_\nu = \begin{pmatrix} 0 & m_D & 0 \\ m_D^T & 0 & M \\ 0 & M^T & \mu \end{pmatrix}, \tag{37}$$

and after block diagonalization the mass matrix for the light neutrino masses can be written as

$$m_\nu = m_D (M^T)^{-1} \mu M^{-1} M_D^T \,. \tag{38}$$

In particular, this matrix can have the required sub-eV neutrino masses for $\mu \simeq 1$ keV and $M \simeq 10^3$ GeV, i.e. for values that are indeed accessible for the present colliders.

Alternatively, one can also explain the very small mass of the neutrinos using *radiative models*. In this case, the tiny magnitude of the masses is explained by introducing new scalars in addition to the particle content of the SM. These new scalars will then be used to generate the neutrino masses through loop diagrams, whereby the loop suppression facilitates explaining the smallness of the neutrino masses. Two well-known examples of the radiative neutrino masses are the Zee model [28], which adds a singlet scalar and an extra Higgs doublet and the Zee-Babu model [29, 30], which adds two singlet scalars.

4.3 The flavour hierarchy problem

The seesaw model that was introduced above is very successful in explaining the smallness of the neutrino masses. However, despite its success in describing the absolute scale of neutrino masses, it still lacks an explanation for another phenomenological problem of the SM, known as the *flavour hierarchy problem*. Indeed, the seesaw mechanism can not explain the hierarchical pattern which emerges when measuring the fermion masses, both for quarks ($m_u, m_d \ll m_c, m_s, \ll m_t, m_b$) as well as for leptons ($m_e \ll m_\mu < m_\tau$). Moreover, if one compares the mixing of leptons, given by the Pontecorvo–Maki–Nakagawa–Sakata (PMNS) matrix to the mixing of quarks, described by the

PoS(CORFU2021)321

Cabibbo-Kobayashi-Maskawa (CKM) matrix, it is evident that, while the mixing of quarks is quite hierarchical ($\theta_{12} \approx 13°$, $\theta_{13} \approx 0.2°$, $\theta_{23} \approx 2.4°$), the leptonic mixing, instead, is almost maximal ($\theta_{12} \approx 34°$, $\theta_{13} \approx 9°$, $\theta_{23} \approx 49°$). Some attempts to explain these features involve extending the symmetry group of the SM by choosing a suitable representation for the leptons under new flavour symmetry groups. More details in this direction can be found in Refs. [31, 32].

4.4 The absolute scale of neutrino masses

Even though the size of neutrino masses is still an open question in theoretical physics, it turns out that constraints on its absolute scale can still be imposed using cosmological and laboratory measurements. In particular, the anisotropies of the CMB spectrum as well as the physics behind large structure formation impose bounds on the sum of neutrino masses. Combining the ΛCDM model with experimental data from WMAP, PLANCK, HST and LSS, the following bound can be obtained [33]

$$\sum_i m_{\nu_i} < 0.14 - 0.72\,\text{eV} \quad (95\%\text{C.L.}) \tag{39}$$

In addition to constraining the sum of the neutrino masses, there are also experiments, trying to measure the neutrino masses separately.[2] For the electron neutrino, most recent measurements of the endpoint of the β-decay spectrum for the tritium decay,

$$^3\text{H} \rightarrow {}^3\text{He} + \text{e}^- + \nu_e\,, \tag{40}$$

at the KATRIN experiment have reported the following upper bound on the electron neutrino mass [34]

$$m_{\nu_e} < 0.9\,\text{eV} \quad (90\%\text{C.L.})\,. \tag{41}$$

The estimated final sensitivity for the KATRIN experiment is,

$$m_{\nu_e} < 0.2\,\text{eV} \quad (90\%\text{C.L.})\,. \tag{42}$$

whereas the final discovery potential of KATRIN within 5σ is limited to neutrino masses above 0.35 eV. Kinematical measurements have also been performed using muon and tau neutrinos. However, the limits obtained in those cases are not competitive with the constraint reported for electron neutrinos by KATRIN.

Another interesting phenomenon that can shed light on neutrino physics is the neutrinoless double β-decay. In order to understand this process, we recall that within the SM it is possible that two neutrons simultaneously turn into two protons, whilst two electrons and two neutrinos are also emitted. This is a very rare process with a lifetime of 10^{21} years, so it is very hard to observe. However, if neutrinos are Majorana fermions, it is also possible that the double β decay occurs without the emission of neutrinos, thus violating lepton number by two units. Since this process (if it exists) has a very long lifetime ($t_{1/2} = 10^{26} - 10^{27}$ years), it has not been observed yet. Nevertheless, an observation of the neutrinoless double beta decay would be a clear evidence that neutrinos are indeed Majorana fermions. The rate of such process is given by

$$\Gamma_{0\nu\beta\beta} = G^{0\nu}\left|M^{0\nu}\right|^2 \left\langle m_{\beta\beta}\right\rangle^2\,, \tag{43}$$

[2] It is important to note that these experiments deal with *flavour eigenstates, i.e.* states with diagonal interaction with the W boson and, as such, these can not rigorously be viewed as states with definite mass.

PoS(CORFU2021)321

where $G^{0\nu}$ and $M^{0\nu}$ are the phase space factor and the nuclear matrix element for the decay, while $\langle m_{\beta\beta} \rangle$ is the effective neutrino mass, depending of the absolute scale of neutrino masses and the elements of the neutrino mixing matrix, including the Majorana phases. For a potential observation, a good separation between the double beta decay spectrum and the neutrinoless double beta decay spectrum is required as well as low background at the neutrinoless double beta decay peak region. If neutrinos are indeed Majorana fermions, various bounds on the mass scale already exist from experiments such as CUORE, EXO-200, GERDA II, KamLAND-ZEN. Moreover, there is an exciting prospect of 3σ discovery for neutrino mass above 20 meV, assuming the neutrino mass spectrum follows the inverted ordering [33].

5. Neutrino oscillations: history and formalism

In this section we will focus on the historical context which lead to the discovery of neutrino oscillations as well as on the description of the basic formalism describing neutrino mixing and neutrino oscillations in vacuum and in matter.

5.1 Historical perspective

The idea of neutrino oscillations was first proposed by Bruno Pontecorvo, who in 1957 suggested the possibility of oscillations between electron neutrino and its antineutrino [35, 36]. Five years later, after the discovery of the muon neutrino, Maki, Nakagawa and Sakata proposed a model with a mixing between the neutrino mass eigenstates ν_1, ν_2 and the flavour eigenstates ν_e, ν_μ [37]:

$$\nu_1 = \nu_e \cos\delta + \nu_\mu \sin\delta \tag{44}$$

$$\nu_2 = -\nu_e \sin\delta + \nu_\mu \cos\delta . \tag{45}$$

Then, due to the presence of the mixing parameter δ, the oscillation phenomenon could happen between the two known flavour eigenstates instead. This was followed up by an explicit calculation of neutrino oscillation probability in vacuum by Pontecorvo and Gribov [38].

Experimentally, the first indication of neutrino oscillations was obtained at the Homestake experiment conducted by Raymond Davis [39]. In this experiment, a large tank was filled with liquid containing ^{37}Cl. Then, once the solar neutrinos (of ν_e flavour) reached the tank, the electron neutrino capture process transformed the ^{37}Cl nuclei into unstable ^{37}Ar nuclei

$$\nu_e + {}^{37}\mathrm{Cl} \rightarrow {}^{37}\mathrm{Ar} + e^- . \tag{46}$$

Then, counting the radioactive decays of the resulting ^{37}Ar nuclei, one could estimate the amount of neutrinos hitting the detector. The results from the experiment were then compared to the Standard Solar Model (SSM), finding that only about one third of the neutrinos expected on the basis of the SSM were actually reaching the detector. Consequently, either the model of the Sun had to be wrong or the experiment had to have been conducted wrong. This discrepancy was also observed by other more modern radiochemical experiments using Gallium (Gallex, GNO, SAGE) and water (Kamiokande, Super-Kamiokande) as target material, although in those cases the reported deficit of solar neutrinos was slightly different: 50% and 40%, respectively. Using all of those results and

PoS(CORFU2021)321

keeping the success of the Standard Model of the Sun in mind, it was clear that some new behaviour of the neutrinos themselves had to be at play. For his contributions in paving the way to this result, Davis received the Nobel Prize in Physics in 2002.

In addition to the solar neutrino problem, there was another anomalous result related to the so-called atmospheric neutrinos. Atmospheric neutrinos are produced when cosmic rays interact with the nuclei present at the Earth atmosphere. Those interactions produce pions and kaons that successively decay into muons, electrons and neutrinos:

$$\pi^- \to \mu^- + \bar{\nu}_\mu \tag{47}$$

$$\mu^- \to e^- + \bar{\nu}_e + \nu_\mu \tag{48}$$

$$\pi^+ \to \mu^+ + \nu_\mu \tag{49}$$

$$\mu^+ \to e^+ + \nu_e + \bar{\nu}_\mu \,. \tag{50}$$

Then, one expects the ratio of muon-neutrinos and electron-neutrinos reaching the Earth to be

$$R_{\mu/e} = \frac{N_{\nu_\mu} + N_{\bar{\nu}_\mu}}{N_{\nu_e} + N_{\bar{\nu}_e}} \simeq 2 \,. \tag{51}$$

However, again, the experimental results by different collaborations turned out to be significantly different from this expectation, since fewer muon neutrinos than expected were measured. The first indication of the deficit in the number of observed the ν_μ was found by the IMB experiment [40]. In 1994, the Kamiokande experiment found that, in addition, this deficit had a dependence on the angle from which the neutrino arrives from [41]. Then, it did not take long for people to realize that the angular dependence is actually a manifestation of the dependence on the distance travelled by the neutrino, since the neutrinos arriving close to overhead had to only traverse the atmosphere while the ones arriving below to the detector had to also pass through the Earth. Finally, in 1998 the discovery of the atmospheric neutrino oscillations ($\nu_\mu \to \nu_\tau$) in Super-Kamiokande was made [42, 43], marking the first time clear evidence of neutrino masses had been found.

Besides these important milestones for the understanding of the neutrino oscillations, a few other important dates should also be remembered. Some of these results will be discussed in more detail in the next chapter.

- In 1987 cosmic neutrinos were detected from Supernova 1987A in Kamiokande [44], IMB and Baksan, providing an important handle on neutrino astrophysics and resulting in a Nobel prize in Physics in 2002 for Masatoshi Koshiba.
- In 2001, the Sudbury Neutrino Observatory (SNO) confirmed a change of flavour in the solar electron-neutrino flux [45].
- In 2002, the KamLAND reactor experiment confirmed that the observed change in flavour occurring for the solar neutrinos was caused by neutrino oscillations [46].
- Between 2011 and 2012, neutrino oscillations were also directly observed in solar, atmospheric, reactor and accelerator physics resulting in the Nobel prize in Physics in 2015 for Takaaki Kajita and Arthur McDonald.

PoS(CORFU2021)321

5.2 Neutrino oscillations in vacuum

In analogy with quarks, the neutrino mixing is described by the 3x3 unitary matrix known as the Pontecorvo-Maki-Nakagawa-Sakata matrix (PMNS). This matrix originates from the fact that the mass eigenstates ($\nu_{\alpha L}$) do not match with the flavour eigenstates (ν_{kL}), but the latter are related to the former via

$$\nu_{\alpha L} = \sum_k U_{\alpha k} \nu_{kL} \,, \tag{52}$$

where $\nu_{\alpha L}$ denotes the flavour eigenstates and ν_{kL} the mass eigenstates. Then, the CC weak leptonic current describing the interaction between flavor neutrinos ν_α and the corresponding charged leptons l_α becomes

$$j_\rho^{CC\,\dagger} = 2 \sum_\alpha \overline{l_{\alpha L}} \gamma_\rho \nu_{\alpha L} = 2 \sum_\alpha \sum_k \overline{l_{\alpha L}} \gamma_\rho U_{\alpha k} \nu_{kL} \,, \tag{53}$$

where the PMNS matrix is given by the rotation matrices between the mass and flavour eigenstates of the charged leptons (U_l) and neutrinos (U_ν) as follows

$$U = U_l^\dagger U_\nu . \tag{54}$$

An important characteristic of the PMNS matrix is the number of free parameters that it entails. As a complex $N \times N$ matrix, it contains a total of $2N^2$ free parameters, of which N^2 can be removed using the condition of unitarity. Then, one is left with N^2 real parameters, which can be classified as $N(N-1)/2$ mixing angles and $N(N+1)/2$ phases, of which not all are physical, however. In particular, note that for the Dirac fields, one can simply perform N phase transformations for the charged lepton fields and $(N-1)$ for the neutrino fields to absorb $(2N-1)$ phases from the PMNS matrix. Quantitatively, redefining

$$l_\alpha \to e^{i\theta_\alpha} l_\alpha , \;\; \nu_k \to e^{i\phi_k} \nu_k , \tag{55}$$

the CC leptonic current becomes

$$j_\rho^{CC\dagger} \to 2 \sum_{\alpha,k} \overline{l_{\alpha L}} e^{-i(\theta_\alpha - \phi_1)} \gamma_\rho U_{\alpha k} e^{i(\phi_k - \phi_1)} \nu_{kL} . \tag{56}$$

The reason why one can only remove $(2N-1)$ phases instead of $2N$ phases is the overall global symmetry associated with the lepton number conservation. Thus, in the end, one is left with $N(N-1)/2$ mixing angles and $(N-1)(N-2)/2$ physical phases.

It is important to emphasize that the phase transformation removing $(2N-1)$ phases from the PMNS is an artefact of the Dirac neutrino scenario. If neutrinos are Majorana fermions instead, the situation will be different, since the Majorana mass terms are not invariant under the global U(1) phase transitions. This is easiest to see considering the effect of the global phase transition

$$\nu_k \to e^{i\phi_k} \nu_k \,, \tag{57}$$

on the neutrino field bilinear:

$$\nu_{kL}^T C^\dagger \nu_{kL} \to e^{2i\phi_k} \nu_{kL}^T C^\dagger \nu_{kL} \,. \tag{58}$$

PoS(CORFU2021)321

Thus, the Majorana neutrino fields can not absorb any phase from the PMNS matrix and only N phases can be rotated away by redefining the charged lepton fields

$$j_\rho^{CC\dagger} \to 2 \sum_{\alpha,k} \overline{l_{\alpha L}} e^{-i\theta_\alpha} \gamma_\rho U_{\alpha k} \nu_{kL} \,, \tag{59}$$

leaving us with $N(N-1)/2$ physical phases for Majorana neutrinos, of which $(N-1)(N-2)/2$ are Dirac phases and $(N-1)$ are Majorana phases. It is also important to note that only the Dirac phases play a role in neutrino oscillations, since Majorana phases only appear in processes where lepton number violation is explicit. Majorana phases are therefore important for the neutrinoless double beta decay.

For two generations, the parametrisation of the mixing matrix depends on one angle only (together with the Majorana phase for Majorana neutrinos, that is not however important for neutrino oscillations) and thus can simply be written as

$$U = \begin{pmatrix} \cos\theta & \sin\theta \\ -\sin\theta & \cos\theta \end{pmatrix} . \tag{60}$$

For three-neutrino generations, the mixing matrix can be described by 3 angles and 1 Dirac (+2 Majorana) CP-violating phase

$$U = \begin{pmatrix} 1 & 0 & 0 \\ 0 & c_{23} & s_{23} \\ 0 & -s_{23} & c_{23} \end{pmatrix} \begin{pmatrix} c_{13} & 0 & s_{13} e^{-i\delta} \\ 0 & 1 & 0 \\ -s_{13} e^{i\delta} & 0 & c_{13} \end{pmatrix} \begin{pmatrix} c_{12} & s_{12} & 0 \\ -s_{12} & c_{12} & 0 \\ 0 & 0 & 1 \end{pmatrix} , \tag{61}$$

where we have divided the PMNS matrix into three contributions each of them responsible for neutrino oscillations in a given sector. The first matrix is used to describe the atmospheric neutrino anomaly and neutrino disappearance at long-baseline experiments, the second one governs the oscillations observed at short-baseline reactor and neutrino appearance long-baseline accelerator experiments and the third one explains the solar neutrino anomaly and the flavour oscillations at long-baseline reactor experiments, such as KamLAND.

Having parametrised neutrino mixing, we now need to understand how one can derive the probablity for neutrino oscillations. To do this, we first recall that the flavour eigenstates of neutrinos are admixtures of the mass eigenstates

$$|\nu_{\alpha L}\rangle = \sum_k U^*_{\alpha k} \, |\nu_{kL}\rangle \ . \tag{62}$$

Then, we consider the time evolution of the neutrino states as given by the Schrödinger equation

$$-i \frac{d}{dt} |\nu\rangle = H \, |\nu\rangle \ . \tag{63}$$

In the mass eigenstate basis the Hamiltonian is diagonal and, therefore, the time evolution of mass eigenstates is simply given by

$$\left|\nu_j\right\rangle \to e^{-iE_j t} \left|\nu_j\right\rangle \ . \tag{64}$$

PoS(CORFU2021)321

In order to further simplify the calculation, one can use the equal momentum approximation, meaning that the momentum of all flavours of neutrinos is assumed to be the same [3]. Then, we have

$$E_j = \sqrt{p_j^2 + m_j^2} \simeq p\sqrt{1 + \frac{m_j^2}{p^2}} \simeq p\left(1 + \frac{1}{2}\frac{m_j^2}{p^2} + ...\right) \simeq p + \frac{m_j^2}{2E}\,, \tag{65}$$

where we used the fact that $m_j/p << 1$ for relativistic neutrinos and that $p \simeq E$ for the same reason. From (65) we see that the energy eigenvalues of the neutrino flavour eigenstates are solely determined by the eigenvalues of the mass matrix. Moreover, for relativistic neutrinos, the time scale is determined by the distance that the neutrinos have travelled (since $v \simeq c$ for relativistic particles) and thus, we can write

$$\left|\nu_j\right\rangle \to e^{-ipL}e^{-i\frac{m_j^2 L}{2E}}\left|\nu_j\right\rangle \to e^{-i\frac{m_j^2 L}{2E}}\left|\nu_j\right\rangle\,. \tag{66}$$

Note that the phase e^{-ipL} has been removed at the last step because it is common for all the neutrino states ν_j and, therefore, does not affect the oscillation probability. Having determined the time evolution of the neutrino mass eigenstates, we proceed now to the calculation of the amplitude for the oscillation between the flavour eigenstates ν_α and ν_β

$$A(\nu_\alpha \to \nu_\beta) = \left\langle \nu_\beta(t)\middle|\nu_\alpha(0)\right\rangle = \sum_j \left\langle \nu_\beta\middle|\nu_j(t)\right\rangle \left\langle \nu_j(t)\middle|\nu_j(0)\right\rangle \left\langle \nu_j(0)\middle|\nu_\alpha\right\rangle\,. \tag{67}$$

where we have used the completeness relation twice. Note that three different stages of the neutrino evolution can be identified in the expression above. The first term from the left corresponds to projecting the final energy eigenstate to the flavour eigenstate. The second one corresponds to the propagation of the initial energy eigenstate and the third one corresponds to projecting the initial neutrino energy eigenstate onto the flavour eigenstate. Writing the flavour eigenstates in terms of the energy eigenstates, it is then easy to see, that the amplitude becomes

$$A(\nu_\alpha \to \nu_\beta) = \sum_j U_{\beta j} e^{-i\frac{m_j^2 L}{2E}} U^*_{\alpha j}\,. \tag{68}$$

The neutrino oscillation probability is then given by the square modulus of this amplitude:

$$P(\nu_\alpha \to \nu_\beta) = \left|\sum_j U_{\beta j} e^{-i\frac{m_j^2 L}{2E}} U^*_{\alpha j}\right|^2\,, \tag{69}$$

which, after some simplification, can be written as

$$\begin{aligned} P(\nu_\alpha \to \nu_\beta) = \delta_{\alpha\beta} - 4\sum_{i\geq j} Re\left(U^*_{\alpha\beta}U_{\alpha j}U_{\beta i}U^*_{\beta j}\right)\sin^2\left(\frac{\Delta m^2_{ij}L}{4E}\right) \\ + 2\sum_{i\geq j} Im\left(U^*_{\alpha i}U_{\alpha j}U_{\beta i}U^*_{\beta j}\right)\sin\left(\frac{\Delta m^2_{ij}L}{2E}\right)\,. \end{aligned} \tag{70}$$

[3] In principle energies and momentum have different values for each of the massive neutrinos considered. An accurate derivation should then consider the neutrino momentum distribution in the neutrino propagation, following a wave-packet treatment. However, since the final result is equivalent, here we have chosen to present a simplified derivation. We refer the interested reader to Ref. [47] for more details on the wave-packet treatment derivation of the neutrino oscillation probability.

PoS(CORFU2021)321

wherein, $\Delta m^2_{ij} = \Delta m^2_i - m^2_j$. A few comments about Eq. (70) are in order.

1. It clearly satisfies conservation of probability: $\sum_\beta P(\nu_\alpha \to \nu_\beta) = 1$.

2. It can also be used for antineutrinos, provided one substitutes U by U^*.

3. Neutrino oscillations violate flavour lepton number conservation but conserve total lepton number.

4. The phases in the mixing matrix induce CP-violation:

$$P(\nu_\alpha \to \nu_\beta) \neq P(\bar{\nu}_\alpha \to \bar{\nu}_\beta)\,. \tag{71}$$

5. Neutrino oscillations are not sensitive to the absolute neutrino mass scale but depend only on the difference of the squared masses Δm^2_{ij}.

6. Neutrino oscillations are not sensitive to the Majorana phases.

We have seen that neutrino oscillations are sensitive to the squared differences of neutrino masses, Δm^2_{ij}. As we will see in the next section, the results of solar experiments and KamLAND provide a precise measurement of Δm^2_{21}. Moreover, the observation of the MSW resonance in solar neutrinos (to be discussed later) has also established its sign, that turns out to be positive. This means that the mass eigenstate ν_1, defined as the state that contains the biggest fraction of ν_e flavour eigenstate, is lighter than ν_2, the state with the second largest fraction of ν_e. On the other hand, atmospheric, long-baseline accelerator and short-baseline reactor experiments determine with good precision the absolute value of the mass splitting Δm^2_{13} that results to be much larger than the previous one. However the sign of Δm^2_{13} is still undetermined. Thus, the mass eigenstate ν_3 defined as the state that contains the least amount of electron neutrino, can be much heavier than the ν_1, ν_2 pair, or much lighter. These two options for the ordering of the neutrino mass spectrum are known as normal ordering and inverted ordering, respectively, see Fig. 1. Current data seem to favor normal ordering, but results are still far from conclusive, so in order to confirm which of these options is realized in Nature, it will be necessary to collect more oscillation data from atmospheric, accelerator and reactor experiments.

Even though we know there are three neutrino families, the existing hierarchy between the measured values of the mass splittings: $\Delta m^2_{12} \simeq 7.5 \times 10^{-5} (eV)^2$ and $|\Delta m^2_{13}| \simeq 2.5 \times 10^{-3} (eV)^2$, as well as the main role played by some of the mixing angles at specific oscillation channels, allows the analysis of experimental neutrino data under the assumption of flavor oscillations between two families. It is important to keep in mind, however, that although this a good approximation, for precision studies one has to consider the presence of all three flavours to perform global analyses of data. Nevertheless, in these notes we present the two-flavour approximation to highlight some important features of neutrino oscillations. Using the neutrino mixing matrix for two generations

$$U = \begin{pmatrix} \cos\theta & \sin\theta \\ -\sin\theta & \cos\theta \end{pmatrix}, \tag{72}$$

PoS(CORFU2021)321

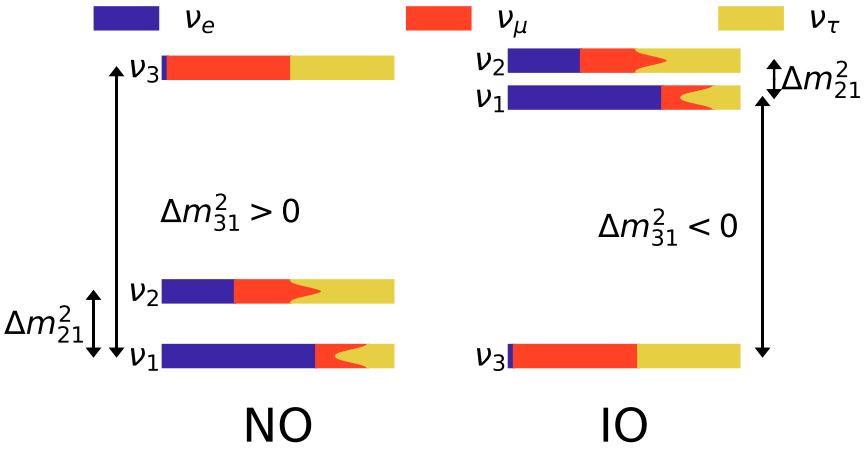

Figure 1: Possible orderings of the neutrino mass spectrum depending on the sign of the atmospheric mass splitting Δm^2_{31}: normal ordering (NO, left) for $\Delta m^2_{31} > 0$ and inverted ordering (IO, right), for $\Delta m^2_{31} < 0$.

the equation for the neutrino oscillation probability, Eq. (70), for two flavours becomes (for $\alpha \neq \beta$)

$$P(\nu_\alpha \to \nu_\beta) = \left| U_{\alpha 1} U^*_{\beta 1} + U_{\alpha 2} U^*_{\beta 2} e^{-i \frac{\Delta m^2_{21}}{2E}} \right|^2 = \sin^2 2\theta \sin^2 \left(\frac{\Delta m^2_{21} L}{4E} \right) . \tag{73}$$

This expression can be understood as an oscillation with amplitude $\sin^2 2\theta$ and phase ϕ, given by

$$\phi = \frac{\Delta m^2_{21} L}{4E} = 1.27 \frac{\Delta m^2_{21}\,[\mathrm{eV}^2] L\,[\mathrm{km}]}{E\,[\mathrm{GeV}]} . \tag{74}$$

Depending on the distance travelled by neutrinos, L, their energy, E, and the squared mass splitting between the different mass eigenstates, Δm^2_{21}, one can distinguish three different regimes for the oscillation phase.

- For short distances, $\phi << 1$, and oscillations cannot develop, so $P_{\alpha\beta} = 0$.
- For long distances, $\phi \simeq 1$, and oscillations are observable.
- For very long distances, $\phi >> 1$, and oscillations are averaged out so that $P_{\alpha\beta} \simeq \sin^2 2\theta$.

5.3 Matter effects for neutrino oscillations

So far we have considered only neutrino oscillations in vacuum. However, neutrino oscillations can be significantly altered in the presence of matter. In particular, when neutrinos pass through matter, the interactions with particles in the medium induce an effective potential for neutrinos. Since neutrinos interact weakly with the SM particles one could expect this effect to be very small. However, in his paper in 1978, Lincoln Wolfenstein showed that the coherent forward scattering amplitude of neutrinos with particles a medium leads to a refraction index for neutrinos that has to be taken into account in their evolution [48]. As a result of this, the mixing between the neutrino flavour

PoS(CORFU2021)321

and mass eigenstates in vacuum will be modified, altering the neutrino oscillation probability with respect to vacuum oscillations. Neutrino interactions with matter are mediated by the gauge bosons of the electroweak sector. To that end, one can distinguish between the neutral current (mediated by the Z boson) and the charged current (mediated by the W boson). To describe these effects we employ an effective field theory formalism and assume that the medium consists of electrons, protons and neutrons. Then, the effective four fermion interaction Hamiltonian can be written as

$$H_{\rm int}^{\nu_\alpha} = \frac{G_F}{\sqrt{2}} \bar{\nu}_\alpha \gamma_\mu (1-\gamma_5) \nu_\alpha \sum_j \bar{f} \gamma_\mu (g_V^{\alpha,f} - g_A^{\alpha,f} \gamma_5) f \,, \tag{75}$$

where G_F denotes the Fermi constant, and $g^{V,A}$ denote the vector and axial couplings, f denotes either the electron, neutron or proton. For the medium that induces the effective potential for neutrinos we make three assumptions:

- We assume that the medium is non-relativistic, so that

$$\left\langle \bar{f} \gamma_\mu f \right\rangle = \frac{1}{2} N_f \, \delta_{\mu 0} \,. \tag{76}$$

- We assume that the medium is unpolarised:

$$\langle f \gamma_5 \gamma^\mu f \rangle = 0 \,. \tag{77}$$

- And we assume that the medium is neutral:

$$N_e = N_p \,, \tag{78}$$

  where $N_e (N_p)$ denotes the number of electrons (protons).

Then, integrating over the f-variables we obtain the matter induced current for the flavour α (last term in Eq. (75))

$$J^{\mu\alpha}_{\rm matter} = \frac{1}{2} \left[N_e \left(g_V^{\alpha,e} + g_V^{\alpha,p} \right) + N_n g_V^{\alpha,n} \right] \,. \tag{79}$$

Using the values of the neutrino couplings to electrons, protons and neutrons given in Table 1, we find

$$J^{\mu\alpha}_{\rm matter} = (N_e - \frac{1}{2} N_n, -\frac{1}{2} N_n, -\frac{1}{2} N_n) \,, \tag{80}$$

from which we can derive the effective potential:

$$V_{\rm matter} = \sqrt{2} G_F \, {\rm diag}(N_e - \frac{1}{2} N_n, -\frac{1}{2} N_n, -\frac{1}{2} N_n) \,. \tag{81}$$

g_V	e^-	p	n
ν_e	$2\sin^2\theta_W + \frac{1}{2}$	$-2\sin^2\theta_W + \frac{1}{2}$	$-\frac{1}{2}$
ν_μ, ν_τ	$2\sin^2\theta_W - \frac{1}{2}$	$2\sin^2\theta_W + \frac{1}{2}$	$-\frac{1}{2}$

Table 1: Vectorial couplings of neutrinos to electrons, protons and neutrons.

PoS(CORFU2021)321

Note that the three neutrino flavours contain the same interaction with the neutron (through the neutral current) and so the neutral current term can be removed from the effective potential by a rephasing of the fields. Then, only the diagonal term for the first generation remains non-zero, showing that the matter effects are important only for ν_e, since this is the only flavour that also has charged current interaction, provided that the only particles present are electrons, protons and neutrons. However, this situation would be different in the presence of sterile neutrinos. In that case, since sterile neutrinos do not interact with the weak currents, the neutral current contribution could not be ignored by a simple rephasing. Finally, we note that for antineutrinos, the effective potential changes sign.

Our task now is to quantify the difference that arises in the oscillation probability due to the matter effects. To start, note that the Hamiltonian in vacuum in the flavour basis (H_f) can be simply deduced from the Hamiltonian in the basis of mass eigenstates (H_m) by a similarity transformation:

$$H_f^{\rm vac} = U H_m U^\dagger = \frac{\Delta m^2}{4E} \begin{pmatrix} -\cos 2\theta & \sin 2\theta \\ \sin 2\theta & \cos 2\theta \end{pmatrix} . \tag{82}$$

Then, the effective Hamiltonian in matter can be written as

$$H^f_{\rm matter} = H_f^{\rm vac} + V_{\rm eff} = \begin{pmatrix} -\frac{\Delta m^2}{4E}\cos 2\theta + V_{CC} & \frac{\Delta m^2}{4E}\sin 2\theta \\ \frac{\Delta m^2}{4E}\sin 2\theta & \frac{\Delta m^2}{4E}\cos 2\theta \end{pmatrix} , \tag{83}$$

where the effective potential induced by the charged current is given by

$$V_{CC} = \sqrt{2} G_F N_e \, . \tag{84}$$

Diagonalizing (83) we can identify the mixing angle and mass splitting in matter and thus write, in analogy to (82),

$$H_f^{\rm matt} = \frac{\Delta M^2}{4E} \begin{pmatrix} -\cos 2\theta_M & \sin 2\theta_M \\ \sin 2\theta_M & \cos 2\theta_M \end{pmatrix} , \tag{85}$$

where now ΔM^2 denotes the splitting between the mass eigenstates in matter (that do not coincide with those in the vacuum) and θ_M denotes the mixing angle in matter. In general, the density of electrons $N_e(x)$ might not be uniform throughout space and so θ_M and ΔM^2 should be calculated for each point in space (or equivalently separately for each point in time). However, in some cases, the computational load can be eased by using analytical approximations.

A good example of a useful approximation is the uniform density approximation. In this case, N_e is taken to be constant throughout space. [4]. Then, θ_M and ΔM^2 are constant as well and need to be calculated only once. Thus, we can use the expression for the oscillation probability in vacuum, Eq. (70), replacing the vacuum parameters with the matter parameters:

$$P(\nu_\alpha \to \nu_\beta) = \sin^2 2\theta_M \sin^2 \left(\frac{\Delta M^2 L}{4E} \right) , \tag{86}$$

[4]Such an approximation could be used for instance for neutrinos traversing the Earth crust.

PoS(CORFU2021)321

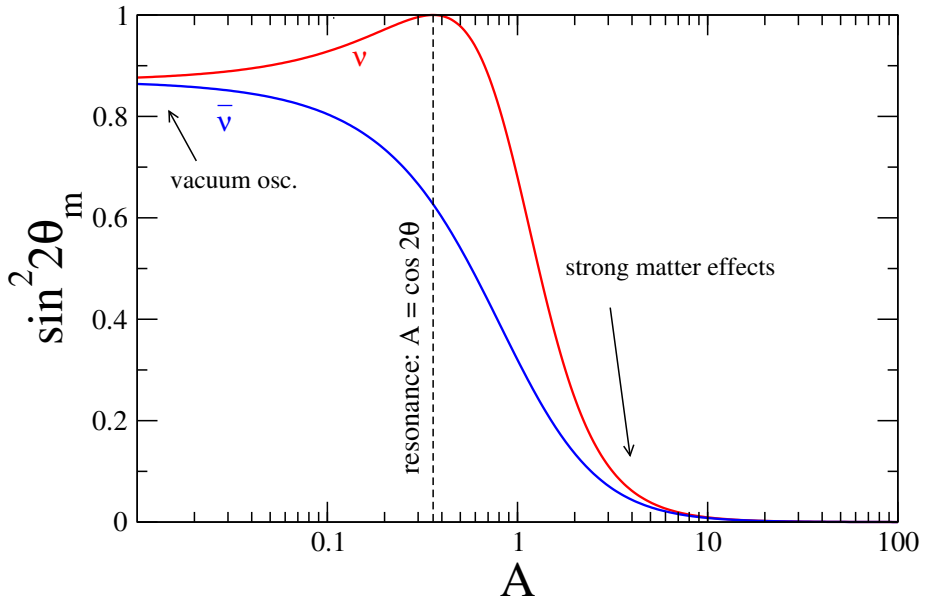

Figure 2: Effective mixing angle in matter θ_m as a function of the parameter A for neutrinos (red line) and antineutrinos (blue line).

where the matter parameters can be written in terms of the vacuum parameters as follows

$$\sin^2 2\theta_M = \frac{\sin^2 2\theta}{\sin^2 2\theta + (\cos 2\theta - A)^2}\,, \tag{87}$$

$$\Delta M^2 = \Delta m^2 \sqrt{\sin^2 2\theta + (\cos 2\theta - A)^2}\,, \tag{88}$$

with

$$A = \frac{2EV}{\Delta m^2}\,. \tag{89}$$

Note that for $A = \cos 2\theta$, the probability gets a resonant enhancement, known as the MSW effect, after Wolfenstein, Mikheyev, Smirnov [48, 49]. The evolution of the mixing angle in matter, θ_m, as a function of A is explicitly displayed for neutrinos and antineutrinos on Fig. 2, where three pertinent regions can be distinguished.

- For $A \ll \cos 2\theta$, matter effects are very small and vacuum oscillations dominate ($\theta_M = \theta$).
- For $A \gg \cos 2\theta$, matter effects dominate and oscillations are suppressed ($\theta_M \approx \pi/2$).
- For $A = \cos 2\theta$, the resonance takes place (only for neutrinos) and the mixing in matter is maximal, $\theta_M \approx \pi/4$, regardless of the value of neutrino mixing in vacuum.

Due to the sign difference for the effective potential of neutrinos and antineutrinos with matter, the resonance condition is satisfied for neutrinos for $\Delta m^2 > 0$ and for antineutrinos for $\Delta m^2 < 0$. As an example, we know that the Sun predominantly produces electron neutrinos. Then, the fact that we see a MSW resonance in the oscillation of the solar neutrinos fixes $\Delta m^2_{21} > 0$.

PoS(CORFU2021)321

Of course, the density of electrons may not be constant in the medium that the neutrinos have to pass through and so often one may want to go beyond the constant matter approximation. In that case, N_e varies with time and thus the diagonalization of $H_{\rm matt}$ has to be performed at every instant to obtain $\theta_M(t)$ and $\Delta M(t)^2$. To describe the evolution of the instantaneous flavour eigenstate in matter, we may then write

$$i\frac{d}{dt}\nu_\alpha = i\frac{d}{dt}\left[U(\theta_M)\nu_i^m\right] = i\frac{d}{dt}U\left(\theta_M\right)\nu_i^m + U(\theta_M)i\frac{d}{dt}\nu_i^m\,, \tag{90}$$

where ν_i^m denotes the instantaneous mass eigenstate in matter. On the other hand, using the Schrödinger equation, we obtain

$$i\frac{d}{dt}\nu_\alpha = H_f\,\nu_\alpha = U(\theta_M)H_{\rm diag}(\Delta M^2)U(\theta_M)^\dagger\nu_\alpha = U(\theta_M)H_{\rm diag}(\Delta M^2)\nu_i^m\,, \tag{91}$$

from which it follows that

$$i\frac{d}{dt}\begin{pmatrix}\nu_1^m\\ \nu_2^m\end{pmatrix} = \begin{pmatrix}-\frac{\Delta M^2}{4E} & -i\dot\theta_M\\ i\dot\theta_M & \frac{\Delta M^2}{4E}\end{pmatrix}\begin{pmatrix}\nu_1^m\\ \nu_2^m\end{pmatrix}\,. \tag{92}$$

Consequently, we see that during their evolution the mass eigenstates get mixed by the off-diagonal terms. However, if

$$\left|\dot\theta_M\right| << \frac{\Delta M^2}{4E}\,, \tag{93}$$

the effect of the off-diagonal terms can be considered small and, in that case, there is no mixing between the two mass eigenstates during their evolution. This is known as the *adiabatic approximation*. The adiabaticity condition can be parametrized by the so-called adiabaticity parameter, defined as

$$\gamma^{-1} \equiv \frac{2\dot\theta_M}{\Delta m^2/2E} = \frac{\sin 2\theta\Delta m^2/2E}{(\Delta M^2/2E)^3}\left|\dot V_{CC}\right| << 1. \tag{94}$$

For instance, the typical value of γ^{-1} inside the Sun is

$$\gamma^{-1} \sim \frac{\Delta m^2}{10^{-9}{\rm eV}^2}\frac{\rm MeV}{E}\,, \tag{95}$$

so that the adiabatic approximation can be applied inside the Sun for neutrino energies up to 10 GeV.

As an example, let us consider the electron neutrinos born at the center of the Sun. Initially, the electron neutrino can be written as a superposition of the mass eigenstates (in the two neutrino approximation)

$$|\nu_e\rangle = \cos\theta_M\left|\nu_1^m\right\rangle + \sin\theta_M\left|\nu_2^m\right\rangle\,. \tag{96}$$

For the solar neutrino experiments that were discussed above, the principal question is what fraction of neutrinos from the Sun actually reach the Earth. To calculate this fraction, we need to add the projection probabilities to both available mass eigenstates. Thus, assuming adiabatic evolution, we have

$$P(\nu_e \to \nu_e) = P_{e1}^{\rm prod}P_{1e}^{\rm det} + P_{e2}^{\rm prod}P_{2e}^{\rm det}\,, \tag{97}$$

PoS(CORFU2021)321

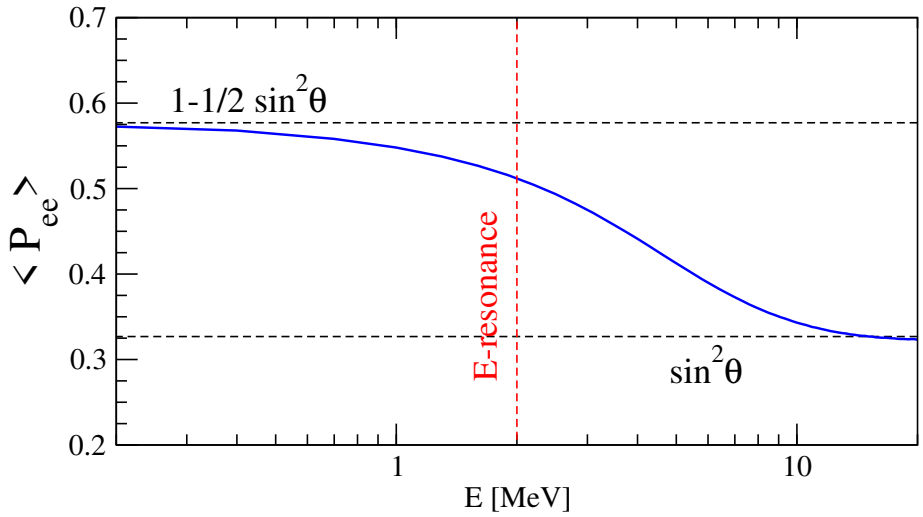

Figure 3: Electron neutrino survival probability as a function of the neutrino energy. The limiting cases corresponding to vacuum oscillations and strong matter effects are displayed for illustration.

where $P_{e1}^{\rm prod}$ represents the squared projection of the initially produced electron neutrino on the first eigenstate, $P_{1e}^{\rm det}$ represents the squared projection of first mass eigenstate onto the finally detected electron neutrino, and so on. The projections needed are given by

$$P_{e1}^{\rm prod} = \cos^2\theta_M\,, \quad P_{1e}^{\rm det} = \cos^2\theta\,, \tag{98}$$

$$P_{e2}^{\rm prod} = \sin^2\theta_M \quad P_{2e}^{\rm det} = \sin^2\theta\,. \tag{99}$$

Thus, the fraction of the electron neutrinos produced in the Sun reaching the Earth is given by

$$P_{ee} = \cos^2\theta_M\cos^2\theta + \sin^2\theta_M\sin^2\theta\,. \tag{100}$$

In the center of the Sun, we have

$$A = \frac{2EV}{\Delta m^2} \simeq 0.2\left(\frac{E}{\rm MeV}\right)\left(\frac{8\times10^{-5}{\rm eV}^2}{\Delta m^2}\right), \tag{101}$$

and the MSW resonance occurs for $A = \cos 2\theta = 0.4$, meaning that $E_{\rm res} \approx 2$ MeV. For lower energies, the vacuum oscillation dominates, and we have

$$P_{ee} = 1 - \frac{1}{2}\sin^2\theta\,, \tag{102}$$

while for higher energies, we have a strong matter effect and

$$P_{ee} = \sin^2\theta\,. \tag{103}$$

For further illustration, the averaged electron neutrino survival probability $\langle P_{ee}\rangle$ as a function of the neutrino energy E is displayed on Fig. 3.

So far, we have exemplified the matter effects inside the Sun. The next natural question that can be asked is if similar effects can also be observed within the Earth. Indeed, it turns out that

PoS(CORFU2021)321

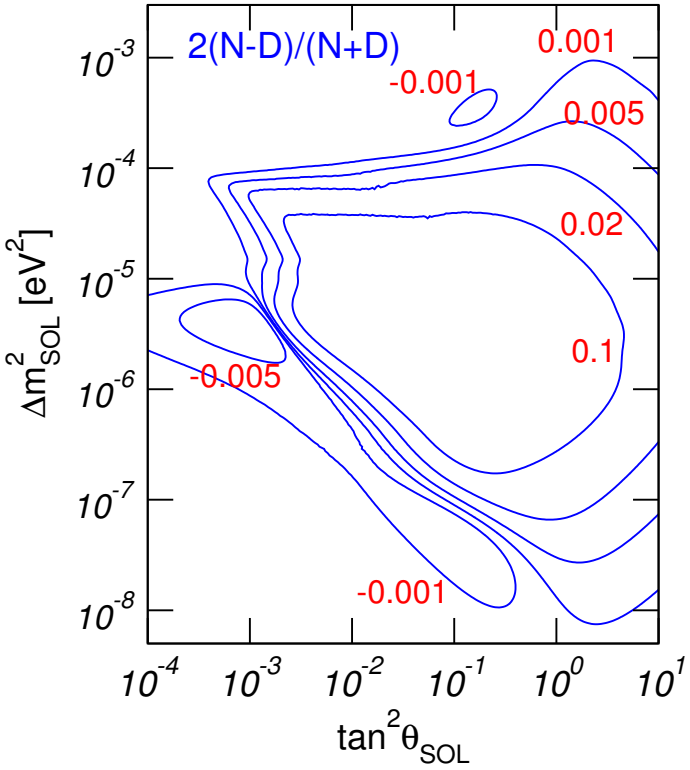

Figure 4: Day-night asymmetry in the solar neutrino flux expected at a terrestrial experiment as a function of the solar mixing parameters.

neutrinos observed during the night are also affected by Earth matter effects. To parameterise this, one can add to the probability during the day ($\sin^2\theta$) the so called regeneration term ($f_{\rm reg}$):

$$P^{\rm det}_{2e} = \sin^2\theta + f_{\rm reg}\,, \tag{104}$$

where

$$f_{\rm reg} = \frac{4EV_{CC}}{\Delta m^2}\sin^2\theta_E \sin^2\left(\frac{\pi L}{L_{\rm osc}}\right)\,. \tag{105}$$

And so, it follows from Eq. (104) that

$$P^{\rm night}_{ee} = P^{\rm day}_{ee} - \cos 2\theta_M\, f_{\rm reg}, \tag{106}$$

yielding the so-called day night asymmetry:

$$A_{DN} \equiv 2\frac{P_N - P_D}{P_N + P_D}. \tag{107}$$

For the actual solar neutrino parameters $f_{\rm reg} \approx 1\%$ and the representative contours are shown on Fig. 4.

In addition to the effect on the solar neutrino propagation, one can also consider how the interaction with matter can alter the oscillation of atmospheric neutrinos. The main oscillation channel for atmospheric neutrinos is $\nu_\mu \to \nu_\tau$, which is not sensitive to matter effects. Nevertheless,

PoS(CORFU2021)321

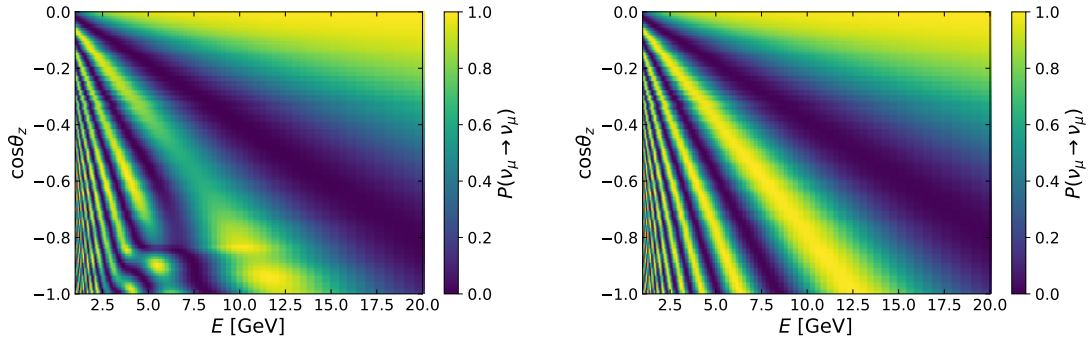

Figure 5: Muon neutrino survival probability as a function of the neutrino energy E and the cosine of the zenith angle $\cos\theta_z$ for normal ordering (left panel) and inverted ordering (right panel). Figure adapted from [50].

for the subdominant oscillation channel $\nu_\mu \to \nu_e$, the MSW resonance can in principle be observed. The matter mixing angle in this case is given by

$$\tan 2\theta_m = \frac{\frac{\Delta m^2}{4E}\sin 2\theta}{\frac{\Delta m^2}{4E}\cos 2\theta \mp \sqrt{2}G_F N_e}\,, \tag{108}$$

with the minus sign for neutrinos and the plus sign for antineutrinos. As it can be seen from the previous expression, matter effects are sensitive to the mass ordering and thus, in principle, can be used to determine the ordering of the neutrino mass spectrum. In particular, for neutrinos with energies in the 3-8 GeV region, the MSW resonance occurs for the normal ordering while for antineutrinos the resonance occurs for the inverted hierarchy as shown in Fig. 5. However, matter effects in atmospheric neutrinos are harder to observe, since they are proportional to the reactor angle, θ_{13}, the smallest of all neutrino mixing angles.

6. Three-neutrino oscillations: experimental results

6.1 Three neutrino oscillations

The oscillation probability for three neutrinos is given by

$$\begin{aligned} P(\nu_\alpha \to \nu_\beta) =& \delta_{\alpha\beta} - 4\sum_{i>j} Re\left(U^*_{\alpha i}U_{\alpha j}U_{\beta i}U^*_{\beta j}\right)\sin^2\left(\frac{\Delta m^2_{ij}L}{4E}\right) \\ &+ 2\sum_{i>j} Im\left(U^*_{\alpha i}U_{\alpha j}U_{\beta i}U^*_{\beta j}\right)\sin\left(\frac{\Delta m^2_{ij}L}{2E}\right), \end{aligned} \tag{109}$$

which depends on the three mixing angles (θ_{12}, θ_{13} and θ_{23}) and the CP phase (δ_{CP}) in the mixing matrix, and the two mass splittings (Δm^2_{21} and Δm^2_{31}). The three mixing angles, the solar mass splitting and the absolute value of the atmospheric one are currently well-measured. However there are still some unknown quantities:

PoS(CORFU2021)321

- **The sign of the atmospheric mass splitting, sign(Δm^2_{31})**, that is, whether m_1 is the lightest neutrino. As discussed in the previous section, we refer to the scenario where $\Delta m^2_{31} > 0$ as normal ordering, whereas the one with $\Delta m^2_{31} < 0$ is the so-called inverted ordering.
- **The octant of θ_{23}**. The mixing angle θ_{23} is known to be close to 45º. It is left to determine whether it is slightly above or below that value. This is relevant for neutrino mass models.
- **The CP phase, δ_{CP}**. There are some indications that CP violation might be maximal but this fact has still to be confirmed.

From experimental data, we know there is a hierarchical relation,

$$|\Delta m^2_{31}| \gg \Delta m^2_{21} \qquad \text{and} \qquad \theta_{13} << 1. \tag{110}$$

This means that three-flavour effects are suppressed and that, in many cases, the dominant oscillations are well-described by effective two-flavour oscillations,

$$P(\nu_\alpha \to \nu_\beta) = \sin^2 2\theta \sin^2 \left(\frac{\Delta m^2 L}{4E} \right) . \tag{111}$$

For instance, solar neutrino experiments and KamLAND data can be well described considering only Δm^2_{21} and θ_{12}. However, a precision measurement of the oscillation parameters requires a full three-neutrino analysis.

6.1.1 Experimental data and methodology

Flavour oscillations have been observed in a large variety of experiments using four different neutrino sources:

- **Solar neutrinos** have been studied in radiochemical experiments using Chlorine (Homestake) [51] or Gallium (Gallex/GNO, SAGE) [52, 53], in the liquid scintillator experiment Borexino [54, 55], in SNO using heavy water [56] and in the water cherenkov detector Super-Kamiokande [57–60].
- Among the experiments studying **reactor neutrinos** one finds KamLAND [61], Double Chooz [62, 63], RENO [64, 65] and Daya Bay [66].
- Concerning **atmospheric neutrinos**, they have been observed in Super-Kamiokande [67, 68], IceCube DeepCore [69, 70], ANTARES [71] and KM3NET/ORCA [72].
- Regarding **accelerator neutrinos**, they were studied in K2K [73] and MINOS [74], and currently in T2K [75] and NOvA [76].

In order to analyse this data, first one needs to calculate the oscillation probabilities taking into account to which channel the experiment is sensitive and if oscillations happen in vacuum or in a certain medium. In order to obtain the expected neutrino signal, one also needs to do a detailed simulation of the experiment, including the size of the detector, its location and efficiency, and many other relevant information. Finally, one needs to compare it with the observed data in the real experiment and perform a statistical analysis in order to obtain the allowed regions in the parameter space.

PoS(CORFU2021)321

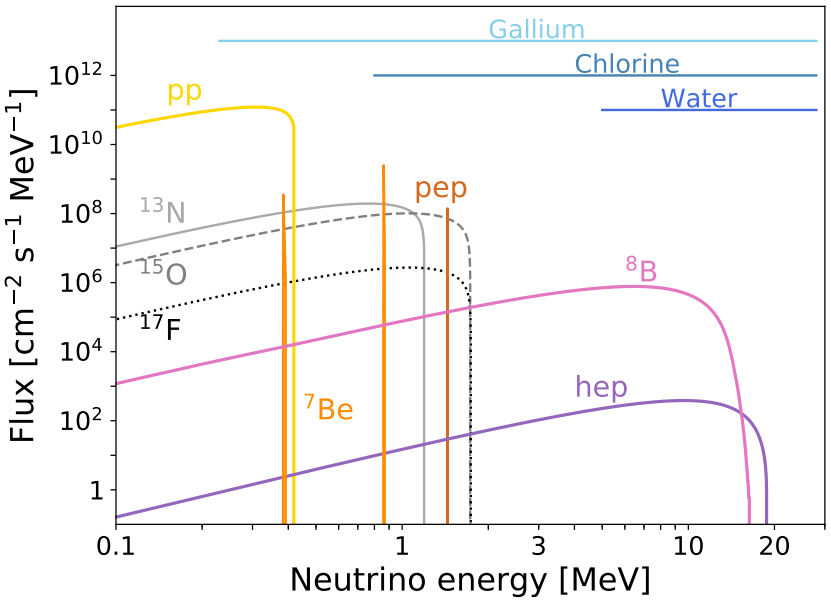

Figure 6: Solar neutrino flux predicted, according to [77–81] as a function of the neutrino energy. The energy range covered by solar neutrinos using Gallium, Chlorine and water is also indicated.

6.2 The solar neutrino sector: $(\Delta m^2_{21}, \sin^2\theta_{12})$

Solar neutrinos are produced in nuclear reactions in the core of the Sun, in the pp and the CNO cycle. We normally refer to the neutrinos produced in each reaction with a different name. For instance, the neutrinos produced in the process $p + p \to d + e^+ + \nu$ are called pp neutrinos. They are the more abundant and also the least energetic ones. Since each process is different, neutrinos are produced with different fluxes and different energy spectra. The Standard Solar Model gives a prediction of the flux of each type of neutrinos that we expect on Earth. The prediction from the Standard Solar Model GS98, as from [77],is shown as an example in Figure 6.

It is important to revisit the solar neutrino problem, considering now why the deficit of neutrinos is different for detectors using Chlorine (∼30 %), Gallium (∼50%) and water (∼40%). One of the reasons is that the experiments see different neutrino flavours. Radiochemical experiments are only sensitive to electron neutrinos, while in Super-Kamiokande the detection process is elastic scattering (ES), $\nu_\alpha + e^- \to \nu_\alpha + e^-$, which is sensitive to all flavours. The second reason is the energy sensitivity of the different experiments. Using Chlorine one can measure neutrinos with E > 0.814 MeV, with Gallium the threshold is E > 0.233 MeV (the only one sensitive to pp neutrinos) while Super-Kamiokande was at first only sensitive to energy above E > 5 MeV. As a consequence, they were observing different neutrino flavour compositions and from different neutrino chains, as shown in Fig. 6. In the third place, one has to account for the energy dependence of the oscillation probability, previously displayed at Fig. 3. Thus, the electron neutrino survival

PoS(CORFU2021)321

probability is larger for low energy neutrinos due to the absence of matter effects

$$P_{ee} = 1 - \frac{1}{2}\sin^2 2\theta \qquad \text{for} \qquad E \lesssim 1\,\text{MeV}\,, \tag{112}$$

and smaller for large energy neutrinos as a consequence of matter effects

$$P_{ee} = \sin^2\theta \qquad \text{for} \qquad E \gtrsim 10\,\text{MeV}\,. \tag{113}$$

Gallium experiments were sensitive to low energy neutrinos, mainly from the pp chain, where $P_{ee} > 0.5$. On the contrary, for the larger energy neutrinos measured with Chlorine and in Super-Kamiokande, the oscillation probability is $\sin^2\theta \sim 0.3$, and that is why a stronger deficit is expected.

One of the experiments that solved the puzzle was the Sudbury Neutrino Observatory (SNO), using heavy water. In addition to measuring elastic scattering (ES), like Super-Kamiokande, and the CC process $\nu_e + d \to p + p + e^-$, SNO could also measure the NC process $\nu_\alpha + d \to p + n + \nu_\alpha$. In SNO, the ratio between the flux measured using CC and NC processes allowed to determine the flux of solar neutrinos in the form of ν_e. Besides that, the total flux of neutrinos of all flavours was determined through the NC process assuming $\phi_{NC}^{SNO} \simeq \phi_{^8B}^{SSM}$. The result obtained was [82]

$$\frac{\phi_{CC}^{SNO}}{\phi_{NC}^{SNO}} = 0.301 \pm 0.033\,, \tag{114}$$

meaning that only 30% of the produced solar neutrinos were detected as ν_e, and the remaining flux was in the form of ν_μ and ν_τ. This was the experiment that show that there was a change of flavour in solar neutrinos and that there was not a deficit of solar neutrinos.

At that point, we knew there was a flavour conversion of ν_e into the other flavours but we didn't know which was the conversion mechanism. The KamLAND experiment was design to study this conversion mechanism. It was a reactor experiment observing electron antineutrinos from 55 commercial nuclear power reactors via inverse beta decay ($\overline{\nu_e} + p \to n + e^+$). The detector was located at an average distance of 180 km from the reactors, which made it sensitive to oscillations with the mass splitting $\Delta m^2 \sim 10^{-5}\text{eV}^2$. If indeed neutrino oscillations were the responsible mechanism for the flavour conversion of solar neutrinos, a deficit of $\overline{\nu}_e$ should also be observed in KamLAND [5]. In 2002, KamLAND presented the first evidence for electron antineutrino disappearance [46], confirming solar neutrino oscillations. Further confirmation came with the results of the spectral distortion in 2004 [85], which clearly showed an oscillation. In 2008, an even clearer measurement of a full 1-oscillation period allowed to determine Δm^2_{21} with great accuracy [86].

The current status of the solar neutrino sector is shown in Fig. 7. One can see how solar data and KamLAND are complementary. The measurement of θ_{12} is dominated by solar neutrino data, whereas KamLAND provides a better measurement of Δm^2_{21}. Notice there is a 2σ mismatch between the best fit point for solar and KamLAND data. Recent results from Super Kamiokande show that the tension is now alleviated although there is still room for a new physics mechanism responsible for this difference.

[5] This statement assumes CPT conservation. For a CPT-violating analysis of neutrino oscillation data see Refs. [83, 84]

PoS(CORFU2021)321

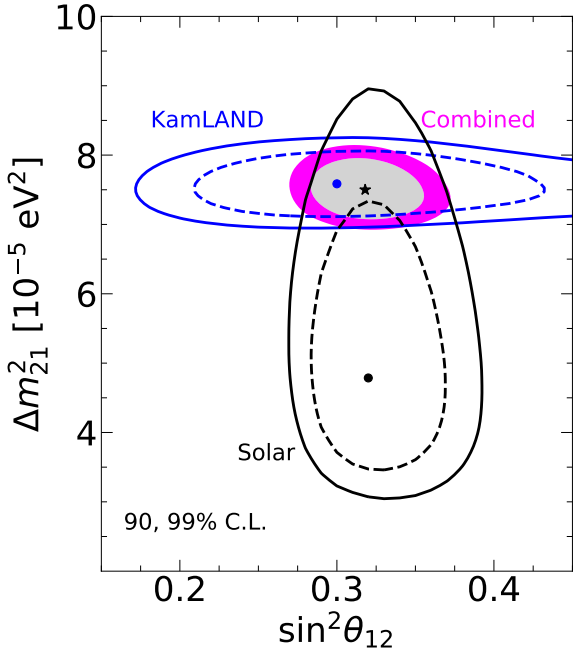

Figure 7: Current status of the solar neutrino sector. Contours correspond to 90 and 99% C.L. (2 d.o.f.). Figure taken from [87] and reproduced with the authorisation of the authors.

6.3 The atmospheric neutrino sector: $(\Delta m^2_{31}, \sin^2\theta_{23})$

In 1998, the first evidence for ν_μ oscillations was found in Super-Kamiokande from the observation of fewer ν_μ in comparison with the expected signal [43]. The deficit showed a dependence on the zenith angle, and consequently, with the distance travelled by neutrinos. This was a clear indication that the deficit was a consequence of neutrino oscillations, since the survival probability for atmospheric ν_μ is approximately given by

$$P_{\mu\mu} = 1 - \sin^2 2\theta_{23} \sin\left(\frac{\Delta m^2_{31} L}{4E_\nu}\right) . \tag{115}$$

With more precise data, in 2004, Super-Kamiokande observed the L/E oscillation pattern that finally confirmed oscillations as the mechanism responsible for the deficit and ruled out other explanations, including decoherence and neutrino decays [88].

In order to constrain the values of the oscillation parameters in the atmospheric neutrino sector, we can use neutrino telescopes, which also observe atmospheric neutrinos. IceCube DeepCore, i.e. an inner and more densely instrumented region of the IceCube detector, is sensitive to neutrinos with energies between 6 and 56 GeV. In the Mediterranean See, ANTARES also measures neutrinos with energies above 20 GeV.

On the other hand, to check the same oscillation channel that gives rise to the deficit of atmospheric neutrinos, a series of long-baseline (LBL) accelerator experiments were designed (MINOS, T2K and NOvA). Their goal was to check the atmospheric anomaly with an artificial source.

PoS(CORFU2021)321

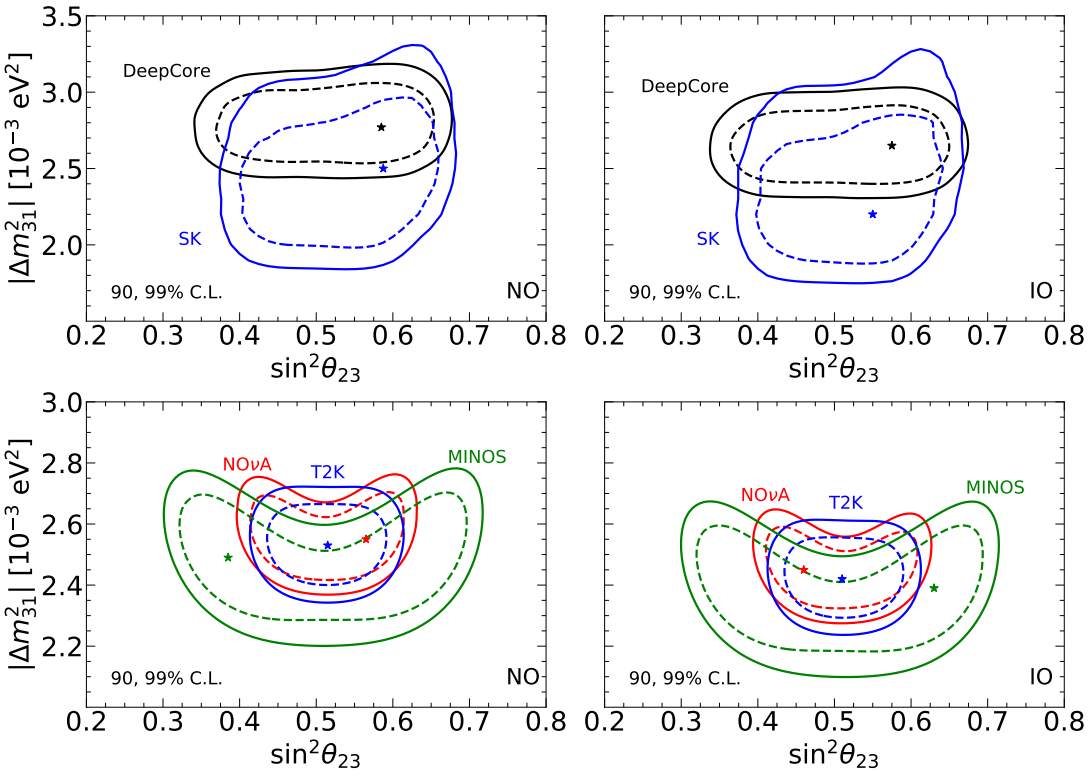

Figure 8: Allowed regions for the atmospheric neutrino oscillations parameters from atmospheric (upper panels) and accelerator data (lower panels) for normal ordering (left) and inverted ordering (right). Contours correspond to 90 and 99% C.L. (2 d.o.f.) [87].

Similarly to the previous case, one can perform a combined analysis of the data from the experiments mentioned above in order to have a more precise measurement of the oscillation parameters. Figure 8 shows the current determination of the oscillation parameters in the atmospheric sector from atmospheric and long-baseline accelerator data.

6.4 The reactor sector: $(\Delta m^2_{31}, \sin^2\theta_{13})$

After the results of CHOOZ [89], which did not find any evidence of electron antineutrino disappearance using a reactor source, a new generation of short-baseline reactor experiments using more powerful reactors and detectors with a larger volumes was designed in order to measure whether θ_{13} was non-zero. They consisted of between 2 and 8 detectors placed at distances between 100 m and 1 km from the reactors. The closest detector was intended to measure the unoscillated flux of electron antineutrinos. The second set of detectors was placed at distances of about 1 km to observe oscillations that manifest as a deficit of $\bar{\nu}_e$s. If all detectors are equal or very similar, the systematics in the flux prediction almost cancel out and the ratio between the number of events in the near and far detector gives essentially a measurement of the oscillation probability,

$$P_{ee} = 1 - \sin^2 2\theta_{13} \sin^2\left(\frac{\delta m^2_{ee} L}{4E}\right) . \tag{116}$$

PoS(CORFU2021)321

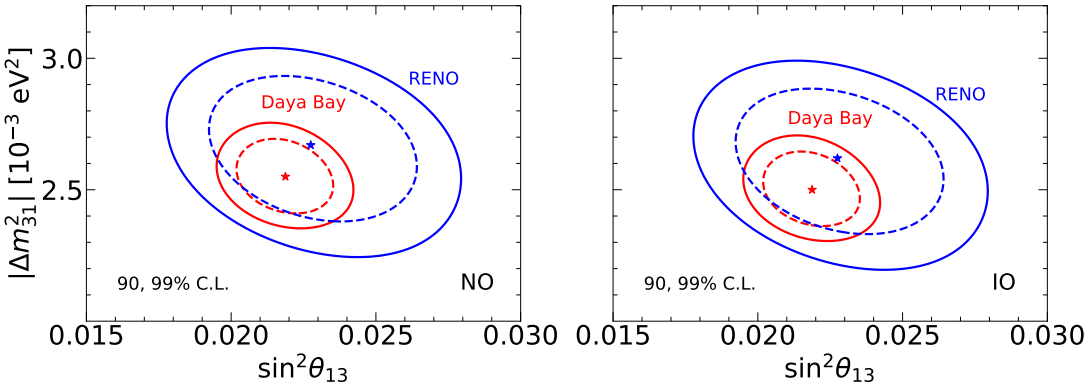

Figure 9: Current status of the reactor neutrino sector for normal ordering (left) and inverted ordering (right). Contours correspond to 90 and 99% C.L. (2 d.o.f.) [87].

There are three experiments of this type, Daya Bay, RENO and Double CHOOZ. The combination of these three experiments gives a precise determination of the oscillation parameters $\sin^2\theta_{13}$ and $|\Delta m^2_{31}|$, although the precision is dominated by Daya Bay [87], as seen in Fig. 9.

6.5 Global fit to oscillation data

Combining and exploiting the complementarity between all the data samples, we manage to put better constraints in the values of the oscillation parameters, summarised in Table 2. The three mixing angles and the mass-splittings have been determined with a precision around 5% or even smaller, although at it was mentioned before, the sing of Δm^2_{31} and the octant of θ_{23} are still unclear. The worst measured parameter is δ_{CP}, with a precision that ranges from 10% to 20% depending on the mass ordering. See [87, 90, 91] for more details on the current status of the determination of the oscillation parameters.

6.5.1 The CP phase

Among the six parameters involved in the three-neutrino oscillation picture, the worst measured parameter is the CP phase since its effects can only be observed in the appearance channel of an experiment. Both Super-Kamiokande atmospheric and accelerator experiments T2K and NOvA are sensitive to the appearance of ν_e (and $\bar{\nu}_e$) in the ν_μ ($\bar{\nu}_\mu$) initial flux. A value of δ_{CP} different from zero and π would lead to an asymmetry between the appearance of electron neutrinos and antineutrinos. From the difference in the oscillation probabilities $P(\nu_\mu \to \nu_e)$ and $P(\bar{\nu}_\mu \to \bar{\nu}_e)$, one can access the value of δ. From Super-K atmospheric analysis [67, 68], there is a preference for maximal CP violation with $\delta = 3\pi/2$ for the best fit in NO. T2K [75] also shows a preference for that same value. Recent results from NOvA [76] show an agreement for maximal CP violation in inverted ordering but a preference for $\delta_{\rm CP} \simeq \pi$ is found for NO. This results in a tension between NOvA and T2K for NO, which makes it difficult to determine the value of δ. Therefore, more experimental data will be necessary to shed light on this matter.

PoS(CORFU2021)321

parameter	best fit ± 1σ	2σ range	3σ range
$\Delta m^2_{21}\,[10^{-5}\text{eV}^2]$	$7.50^{+0.22}_{-0.20}$	7.12–7.93	6.94–8.14
$\lvert\Delta m^2_{31}\rvert\,[10^{-3}\text{eV}^2]$ (NO)	$2.55^{+0.02}_{-0.03}$	2.49–2.60	2.47–2.63
$\lvert\Delta m^2_{31}\rvert\,[10^{-3}\text{eV}^2]$ (IO)	$2.45^{+0.02}_{-0.03}$	2.39–2.50	2.37–2.53
$\sin^2\theta_{12}/10^{-1}$	3.18 ± 0.16	2.86–3.52	2.71–3.69
$\sin^2\theta_{23}/10^{-1}$ (NO)	5.74 ± 0.14	5.41–5.99	4.34–6.10
$\sin^2\theta_{23}/10^{-1}$ (IO)	$5.78^{+0.10}_{-0.17}$	5.41–5.98	4.33–6.08
$\sin^2\theta_{13}/10^{-2}$ (NO)	$2.200^{+0.069}_{-0.062}$	2.069–2.337	2.000–2.405 d
$\sin^2\theta_{13}/10^{-2}$ (IO)	$2.225^{+0.064}_{-0.070}$	2.086–2.356	2.018–2.424
δ/π (NO)	$1.08^{+0.13}_{-0.12}$	0.84–1.42	0.71–1.99
δ/π (IO)	$1.58^{+0.15}_{-0.16}$	1.26–1.85	1.11–1.96

Table 2: Neutrino oscillation parameters summary determined from the global analysis in [87]. The intervals quoted for inverted ordering refer to the local minimum for this neutrino mass ordering. See also [90, 91] for similar analyses.

7. Neutrino oscillations beyond three-neutrino flavour oscillations

According to the measurement of the invisible decay of the Z boson at LEP, there are only three light active neutrinos. However, there are some experimental hints pointing towards the existence of a fourth sterile neutrino.

The first one is a historical signal at the LSND experiment in the channel of electron neutrino appearance ($\nu_\mu \to \nu_e$) at a ratio $L/E \sim 1$ eV^2 [92]. Given the values of Δm^2_{21} and Δm^2_{31} measured, such a large mass splitting can not be accommodated within the three-neutrino picture. Thus, one needs an additional sterile neutrino to explain the observed signal. Later on, the MiniBooNE experiment was built to test the LSND anomaly, searching for $\nu_\mu \to \nu_e$ and $\bar\nu_\mu \to \bar\nu_e$ at a similar L/E ratio. MiniBooNE also reported anomalous results and could not reject the sterile neutrino hypothesis, meaning that the signal could also be explained with a sterile neutrino with $\Delta m^2_{41} \sim 1$ eV^2 [93].

Besides MiniBooNE and LSND, there is also the so-called *reactor antineutrino anomaly*. In very short baseline reactor experiments, a neutrino deficit was found after reevaluating the theoretical predictions for the reactor $\bar\nu_e$ fluxes. This result could also be interpreted as the disappearance of reactor antineutrinos due to flavour oscillations with a mass splitting $\Delta m^2_{41} \sim 1$ eV^2 [94, 95]. Finally, there is an anomalous result reported after the calibration of Gallium solar neutrino experiments with radioactive sources. During the calibration, a deficit of ν_e was observed, compared to the predictions. This deficit, known as the *Gallium anomaly*, which happened over distances of 1 m,

PoS(CORFU2021)321

can also be explained with a sterile neutrino with a mass splitting of the same order of magnitude [52, 96, 97]. Such deficit was recently confirmed by the BEST experiment [98].

Hence, there are four experimental hints that could be interpreted as the existence of a fourth sterile neutrino. A sterile neutrino is nothing but a fermion singlet of the Standard Model. It has no interactions, except maybe with the Higgs boson (in order to have a mass), with active neutrinos or some additional interactions beyond the SM. The motivation for sterile neutrinos is quite wide. Sterile neutrinos with masses of order of the eV could explain the experimental anomalies presented above. Much heavier sterile neutrinos (TeV - $M_{\rm Planck}$) could be responsible for the smallness of the active neutrino masses (for instance, in the seesaw mechanism) and may provide an explanation for the baryon asymmetry of the Universe, generated via leptogenesis. In addition, they could also be part of the dark matter of the Universe. From these point on, we will focus on light sterile neutrinos and their relation with the experimental anomalies.

It is possible to perform a combined analysis of all the neutrino oscillation data considering three active neutrinos and a sterile one. This is often referred as the 3+1 framework or neutrino scheme. Although there are some hints that support the existence of a sterile neutrino, some other experiments have not seen any sign of them, even in the same region of the parameter space. For instance, many disappearance experiments (CDHS, MINOS/MINOS+[99, 100], IceCube [101, 102], Super-Kamiokande) do not see any signal. Hence, there is a strong tension between the appearance experiments (LSND and MiniBooNE) and the ones looking at the disappearance channels. As a result, the quality of the combined fit is very bad [103, 104]. Currently, the MicroBooNE experiment is taking and analysing data in order to confirm or reject the results from MiniBooNE and LSND. In the light of the latest results presented, no conclusion can be drawn.

The tension between oscillation experiments is not the only one. In cosmology, neutrinos with masses of the order of 1 eV would contribute to the sum of neutrino masses $\sum m_\nu$ and to the effective number of relativistic species ($N_{\rm eff}$), as measured from CMB and structure formation. It is possible to accommodate a light sterile neutrino in the picture as long as the mixing between active and sterile neutrinos is small. However, for the mass and mixing required in order to explain the experimental anomalies, the sterile neutrino would be fully thermalised in the early universe [105]. In that case, $N_{\rm eff} \sim 4$ and the sum of neutrino masses would be $\sum m_\nu \gtrsim 0.05{\rm eV} + \sqrt{\Delta m^2_{41}} \gtrsim 1{\rm eV}$. Current constraints from cosmology limit the sum of neutrino masses to $\sum m_\nu < 0.12 - 0.60$ eV [106], depending on the datasets included and some of the underlying assumptions. On the other hand, according to Planck data, $N = 2.99 \pm 0.17$ [106]. Hence, some model building would be required in order to accommodate eV-sterile neutrinos with the cosmological observations.

8. Neutrino physics beyond the Standard Model

Neutrino results suggest the presence of Beyond the Standard Model (BSM) physics, since one needs to explain

- Light neutrino masses. To do that, one needs to introduce a mass generation mechanism.
- The large neutrino mixing, compared to the quark sector. This is known as the flavour problem.

PoS(CORFU2021)321

- The short-baseline anomalies that lead to the proposal of eV-sterile neutrinos.

Many BSM physics scenarios have been addressed in the literature, among which one finds neutrino non-standard interactions (NSI) with matter, exotic electromagnetic neutrino properties, the presence of light sterile neutrinos, the mixing with heavy sterile neutrinos leading to non-unitary three neutrino mixing and Lorentz and CPT invariance violation.

8.1 Neutrino non-standard interactions

Neutrino non-standard interactions appear in models of neutrino masses. Such interactions can be classified into neutral current NSI and charged-current NSI, and can lead, for instance, to flavour-changing neutral current processes or to the breaking of the lepton flavour universality of the SM interactions. If one allows for the presence of NSI in the analysis of neutrino oscillation data, the precision with which the parameters are measured becomes much worse. This is due to the fact that there can be degeneracies between the oscillation parameters and the couplings responsible for these new interactions. Besides that, NSI would also affect the sensitivity reach of future experiments. As an example, in the case of solar neutrinos, if one allows for non-zero NSI, it is possible to find two solutions for the mixing angle θ_{12}: one with $\theta_{12} < \pi/4$ (the standard one) and another with $\theta_{12} > \pi/4$ [107]. In the case of the future DUNE experiment, its sensitivity to the atmospheric mixing angle θ_{23} would also worsen if a non-zero NSI were allowed in the analysis [108]. For a recent review on neutrino non-standard interactions, see [109].

8.2 Non-unitary three neutrino mixing

Many models of neutrino masses introduce heavy states that mix with the light active neutrinos. Then, one would have a dimension N unitary mixing matrix, whereas the 3×3 mixing matrix accessible at low-energy experiments would not be unitary any more. In that case, one can parametrise the 3×3 non-unitary mixing matrix as follows [110],

$$N = \begin{pmatrix} \alpha_{11} & 0 & 0 \\ \alpha_{21} & \alpha_{22} & 0 \\ \alpha_{31} & \alpha_{32} & \alpha_{33} \end{pmatrix} U^{3\times 3} \,, \tag{117}$$

where $U^{3\times 3}$ is the standard PMNS neutrino mixing matrix. In this case, we need 9 additional parameters (3 real diagonal parameters α_{ii} plus 3 complex non-diagonal parameters α_{ij}) to describe the light neutrino mixing and, as it has been shown, the sensitivity of future experiments might be compromised. For instance, the measurement of the CP phase in DUNE could be expoiled in this scenario [111].

8.3 Lorentz and CPT invariance violation

Lorentz and CPT symmetries are the basis for local relativistic quantum field theories. Motivated by current and future high-precision experiments, one may try to probe such symmetries. In fact, the observation of CPT or Lorentz invariance violation would be a sign of new physics, for instance Quantum Gravity or String Theories.

PoS(CORFU2021)321

The Standard Model Extension (SME) [112–114] is an extension of the Standard Model Lagrangian which allows for CPT and Lorentz invariance violation while preserving all the remaining symmetries of the Standard Model and ensuring that the Lagrangian still transforms as a scalar. In this framework, the neutrino sector is described by

$$\mathcal{L} = \frac{1}{2}\bar{\psi}\left(i\gamma^{\alpha}\partial_{\alpha} + M + Q\right)\psi\,, \tag{118}$$

where Q contains all the Lorentz violating operators.

The Lorentz invariance violating (LIV) term of the Lagrangian can be parametrised as [115, 116],

$$\mathcal{L}_{\rm LIV} = -\frac{1}{2}\left[a^{\mu}_{\alpha\beta}\bar{\psi}\gamma_{\mu}\psi + b^{\mu}_{\alpha\beta}\bar{\psi}_{\alpha}\gamma_5\gamma_{\mu}\psi_{\beta} + c^{\mu\nu}_{\alpha\beta}\bar{\psi}\gamma_{\mu}\partial_{\nu}\psi + d^{\mu\nu}_{\alpha\beta}\bar{\psi}_{\alpha}\gamma_5\gamma_{\mu}\partial_{\nu}\psi_{\beta}\right] + \text{h.c.} \tag{119}$$

and the observable effect on the left-handed neutrinos is controlled by

$$(a_L)^{\mu}_{\alpha\beta} = (a+b)^{\mu}_{\alpha\beta} \quad \text{and} \quad (c_L)^{\mu}_{\alpha\beta} = (c+d)^{\mu}_{\alpha\beta}\,. \tag{120}$$

This scenario has been explored in the context of many neutrino oscillation experiments like MINOS [117], IceCube [118] or SNO [119]. The effective neutrino Hamiltonian in this scenario is given by $H = H_{\rm vac} + H_{\rm mat} + H_{\rm LIV}$, where $H_{\rm vac}$ is the Hamiltonian in vacuum, $H_{\rm mat}$ is the term accounting for neutrino interactions with matter, and $H_{\rm LIV}$ encodes the possible isotropic Lorentz invariance violation and is of the form

$$H_{\rm LIV} = \begin{pmatrix} a_{ee} & a_{e\mu} & a_{e\tau} \\ a^*_{e\mu} & a_{\mu\mu} & a_{\mu\tau} \\ a^*_{e\tau} & a^*_{\mu\tau} & a_{\tau\tau} \end{pmatrix} - \frac{4}{3}E\begin{pmatrix} c_{ee} & c_{e\mu} & c_{e\tau} \\ c^*_{e\mu} & c_{\mu\mu} & c_{\mu\tau} \\ c^*_{e\tau} & c^*_{\mu\tau} & c_{\tau\tau} \end{pmatrix}, \tag{121}$$

where we have adopted the short-hand notation $a_{\alpha\beta} = (a_L)^0_{\alpha\beta}$ and $c_{\alpha\beta} = (c_L)^0_{\alpha\beta}$. The coefficients $c_{\alpha\beta}$ have been strongly constrained with atmospheric data, whereas the constraints in the CPT-odd part of the Hamiltonian, given by the coefficients $a_{\alpha\beta}$, will be improved by DUNE thanks to the modification of the electron neutrino appearance probability in the presence of LIV [120].

Regarding the CPT symmetry, it is currently presented as an exact symmetry in nature. However, from a historical point of view, parity and CP were also considered exact symmetries of nature in the past, until experimental evidence proved that they were not. If CPT were not conserved, then $P(\nu_\alpha \to \nu_\beta) \neq P(\bar{\nu}_\beta \to \bar{\nu}_\alpha)$. Then, flavour oscillations can be used to constrain CPT violation in the neutrino sector.

One way to test CPT invariance is to assume that neutrinos and antineutrinos are ruled by different sets of oscillation parameters. For instance, T2K performed a separate analysis for neutrinos and antineutrinos and found different best fit values for the neutrino (θ_{23}, Δm^2_{32}) and antineutrino parameters ($\bar{\theta}_{23}$, $\Delta\bar{m}^2_{32}$), although the results were consistent with CPT conservation [121]. From global analyses of oscillation data, the bounds read [83]

$$\begin{aligned} &|\Delta m^2_{21} - \Delta\bar{m}^2_{21}| < 4.7\times10^{-5}\ \text{eV}^2 \qquad &&|\sin^2\theta_{12} - \sin^2\bar{\theta}_{12}| < 0.14 \\ &|\Delta m^2_{31} - \Delta\bar{m}^2_{31}| < 3.7\times10^{-4}\ \text{eV}^2 \qquad &&|\sin^2\theta_{13} - \sin^2\bar{\theta}_{13}| < 0.03 \\ & &&|\sin^2\theta_{32} - \sin^2\bar{\theta}_{23}| < 0.32\ . \end{aligned}$$

PoS(CORFU2021)321

DUNE is expected to improve some of these bounds, in particular, the limits on $|\Delta m^2_{31} - \Delta\bar{m}^2_{31}|$ by one order of magnitude [83].

It is also important to point out that, if CPT is violated but one performs a combined analysis of neutrino and antineutrino data, one can obtain imposter solutions. A combined fit would still give a best fit value that could explain relatively well neutrino and antineutrino data. However, this best fit would not be true value of the oscillation parameters. Moreover, one could even exclude with significance the true values of the parameters [83]. This is why, even if it is well justified to performed global analysis assuming CPT conservation, one should keep in mind that if CPT is violated, their results would have to be revisited.

9. Summary

In these lectures, we have covered the main aspects of neutrino phenomenology . Neutrinos play an important role in many physical and astrophysical scenarios and this is why it is important to study neutrino properties. Important discoveries in neutrino physics along the last centuries have provided the first evidence for physics beyond the Standard Model: neutrino masses. Extensions of the Standard Model are needed to explain the smallness of neutrino masses and also to understand the flavour structure and the differences in mixing between neutrinos and quarks.

Regarding the absolute neutrino mass scale, there are some bounds from cosmological and laboratory experiments pointing towards the fact that the fact the lightest neutrino mass is below the electronvolt. More information on neutrino masses can be obtained from the study of neutrino oscillations. Flavour oscillations are a well-established phenomenon which has been observed in several experiments, with natural (from the Sun and the atmosphere) and artificial sources (reactor and accelerators). Combining the available experimental data, most of the oscillation parameters have been measured quite accurately (with a precision $\lesssim 5$ %), except for the CP -violating phase. With respect to the unknowns in the three-neutrino oscillation picture, there are indications pointing towards normal ordering and maximal CP violation but those still need to be confirmed by current and future experiments.

Several anomalous results seem to indicate the existence of light sterile neutrinos, with a mass splitting $\Delta m^2_{41} \sim 1$ eV. However, these hints are in conflict with other data. For instance, LSND and MiniBooNE disagree with negative signals in ν_μ disappearance searches. Also, there is no consistent picture of eV-sterile neutrinos and cosmology, since such a sterile neutrino is in serious tension with current data.

That is not the only beyond the standard model scenario that has been studied in the literature. There are many others, such as the presence of non-standard neutrino interactions or the non-unitarity of the three neutrino mixing matrix, which may affect considerably the precision of future experiments.

Finally, some scenarios motivated by quantum gravity phenomenology have been reviewed, for instance, the violation of Lorentz and CPT invariance.

PoS(CORFU2021)321

Acknowledgements

The authors would like to acknowledge networking support by the COST Action CA18108. PMM and MT acknowledge financial support from the Spanish grants PID2020-113775GB-I00 (AEI / 10.13039/501100011033) and PROMETEO/2018/165 (Generalitat Valenciana). PMM is supported by FPU18/04571.

References

[1] H. Bethe and R. Peierls. The 'neutrino'. *Nature*, 133:532, 1934.

[2] F. Reines. Foreword to "Spaceship Neutrino" by Christine Sutton. page xi, 1992.

[3] C. L. Cowan, F. Reines, F. B. Harrison, H. W. Kruse, and A. D. McGuire. Detection of the free neutrino: A Confirmation. *Science*, 124:103–104, 1956.

[4] B. Pontecorvo. Electron and Muon Neutrinos. *Zh. Eksp. Teor. Fiz.*, 37:1751–1757, 1959.

[5] M. Schwartz. Feasibility of using high-energy neutrinos to study the weak interactions. *Phys. Rev. Lett.*, 4:306–307, 1960.

[6] G. Danby, J. M. Gaillard, Konstantin A. Goulianos, L. M. Lederman, Nari B. Mistry, M. Schwartz, and J. Steinberger. Observation of High-Energy Neutrino Reactions and the Existence of Two Kinds of Neutrinos. *Phys. Rev. Lett.*, 9:36–44, 1962.

[7] Salvatore Mele. The Measurement of the Number of Light Neutrino Species at LEP. *Adv. Ser. Direct. High Energy Phys.*, 23:89–106, 2015.

[8] K. Kodama et al. Observation of tau neutrino interactions. *Phys. Lett. B*, 504:218–224, 2001.

[9] T. D. Lee and Chen-Ning Yang. Question of Parity Conservation in Weak Interactions. *Phys. Rev.*, 104:254–258, 1956.

[10] C. S. Wu, E. Ambler, R. W. Hayward, D. D. Hoppes, and R. P. Hudson. Experimental Test of Parity Conservation in β Decay. *Phys. Rev.*, 105:1413–1414, 1957.

[11] M. Goldhaber, L. Grodzins, and A. W. Sunyar. Helicity of Neutrinos. *Phys. Rev.*, 109:1015–1017, 1958.

[12] S. L. Glashow. Partial Symmetries of Weak Interactions. *Nucl. Phys.*, 22:579–588, 1961.

[13] Steven Weinberg. A Model of Leptons. *Phys. Rev. Lett.*, 19:1264–1266, 1967.

[14] F. J. Hasert et al. Observation of Neutrino Like Interactions Without Muon Or Electron in the Gargamelle Neutrino Experiment. *Phys. Lett. B*, 46:138–140, 1973.

[15] Steven Weinberg. Baryon and Lepton Nonconserving Processes. *Phys.Rev.Lett.*, 43:1566–1570, 1979.

PoS(CORFU2021)321

[16] M. Fukugita and T. Yanagida. Baryogenesis Without Grand Unification. *Phys. Lett. B*, 174:45–47, 1986.

[17] Peter Minkowski. $\mu \to e\gamma$ at a Rate of One Out of 1-Billion Muon Decays? *Phys.Lett.*, B67:421, 1977.

[18] Murray Gell-Mann, Pierre Ramond, and Richard Slansky. Complex Spinors and Unified Theories. *Conf.Proc.*, C790927:315–321, 1979.

[19] Tsutomu Yanagida. Horizontal Symmetry and Masses of Neutrinos. *Conf.Proc.*, C7902131:95–99, 1979.

[20] Rabindra N. Mohapatra and Goran Senjanovic. Neutrino Mass and Spontaneous Parity Violation. *Phys.Rev.Lett.*, 44:912, 1980.

[21] J. Schechter and J.W.F. Valle. Neutrino Masses in SU(2) x U(1) Theories. *Phys.Rev.*, D22:2227, 1980.

[22] George Lazarides, Q. Shafi, and C. Wetterich. Proton Lifetime and Fermion Masses in an SO(10) Model. *Nucl. Phys. B*, 181:287–300, 1981.

[23] T. P. Cheng and Ling-Fong Li. Neutrino Masses, Mixings and Oscillations in SU(2) x U(1) Models of Electroweak Interactions. *Phys. Rev. D*, 22:2860, 1980.

[24] M. Magg and C. Wetterich. Neutrino Mass Problem and Gauge Hierarchy. *Phys. Lett. B*, 94:61–64, 1980.

[25] Rabindra N. Mohapatra and Goran Senjanovic. Neutrino Masses and Mixings in Gauge Models with Spontaneous Parity Violation. *Phys. Rev. D*, 23:165, 1981.

[26] Robert Foot, H. Lew, X.G. He, and Girish C. Joshi. Seesaw Neutrino Masses Induced by a Triplet of Leptons. *Z.Phys.*, C44:441, 1989.

[27] R. N. Mohapatra and J. W. F. Valle. Neutrino Mass and Baryon Number Nonconservation in Superstring Models. *Phys. Rev. D*, 34:1642, 1986.

[28] A. Zee. A Theory of Lepton Number Violation, Neutrino Majorana Mass, and Oscillation. *Phys. Lett. B*, 93:389, 1980. [Erratum: Phys.Lett.B 95, 461 (1980)].

[29] A. Zee. Quantum Numbers of Majorana Neutrino Masses. *Nucl. Phys. B*, 264:99–110, 1986.

[30] K. S. Babu. Model of 'Calculable' Majorana Neutrino Masses. *Phys. Lett. B*, 203:132–136, 1988.

[31] Guido Altarelli and Ferruccio Feruglio. Discrete Flavor Symmetries and Models of Neutrino Mixing. *Rev. Mod. Phys.*, 82:2701–2729, 2010.

[32] Hajime Ishimori, Tatsuo Kobayashi, Hiroshi Ohki, Yusuke Shimizu, Hiroshi Okada, and Morimitsu Tanimoto. Non-Abelian Discrete Symmetries in Particle Physics. *Prog. Theor. Phys. Suppl.*, 183:1–163, 2010.

PoS(CORFU2021)321

[33] Massimiliano Lattanzi and Martina Gerbino. Status of neutrino properties and future prospects - Cosmological and astrophysical constraints. *Front. in Phys.*, 5:70, 2018.

[34] M. Aker et al. Direct neutrino-mass measurement with sub-electronvolt sensitivity. *Nature Phys.*, 18(2):160–166, 2022.

[35] B. Pontecorvo. Inverse beta processes and nonconservation of lepton charge. *Zh. Eksp. Teor. Fiz.*, 34:247, 1957.

[36] B. Pontecorvo. Mesonium and anti-mesonium. *Sov. Phys. JETP*, 6:429, 1957.

[37] Ziro Maki, Masami Nakagawa, and Shoichi Sakata. Remarks on the unified model of elementary particles. *Prog. Theor. Phys.*, 28:870–880, 1962.

[38] V. N. Gribov and B. Pontecorvo. Neutrino astronomy and lepton charge. *Phys. Lett. B*, 28:493, 1969.

[39] Raymond Davis, Jr., Don S. Harmer, and Kenneth C. Hoffman. Search for neutrinos from the sun. *Phys. Rev. Lett.*, 20:1205–1209, 1968.

[40] J. M. LoSecco et al. Test of Neutrino Oscillations Using Atmospheric Neutrinos. *Phys. Rev. Lett.*, 54:2299, 1985.

[41] K. S. Hirata et al. Observation of a small atmospheric muon-neutrino / electron-neutrino ratio in Kamiokande. *Phys. Lett. B*, 280:146–152, 1992.

[42] Takaaki Kajita. Atmospheric neutrino results from Super-Kamiokande and Kamiokande: Evidence for neutrino(mu) oscillations. *Nucl. Phys. B Proc. Suppl.*, 77:123–132, 1999.

[43] Y. Fukuda et al. Evidence for oscillation of atmospheric neutrinos. *Phys. Rev. Lett.*, 81:1562–1567, 1998.

[44] K. S. Hirata et al. Observation in the Kamiokande-II Detector of the Neutrino Burst from Supernova SN 1987a. *Phys. Rev. D*, 38:448–458, 1988.

[45] Q. R. Ahmad et al. Measurement of the rate of $\nu_e + d \rightarrow p + p + e^-$ interactions produced by ^{8}B solar neutrinos at the Sudbury Neutrino Observatory. *Phys. Rev. Lett.*, 87:071301, 2001.

[46] K. Eguchi et al. First results from KamLAND: Evidence for reactor anti-neutrino disappearance. *Phys. Rev. Lett.*, 90:021802, 2003.

[47] Carlo Giunti and Chung W. Kim. *Fundamentals of Neutrino Physics and Astrophysics*. 2007.

[48] L. Wolfenstein. Neutrino Oscillations in Matter. *Phys. Rev. D*, 17:2369–2374, 1978.

[49] S. P. Mikheev and A. Yu. Smirnov. Resonant amplification of neutrino oscillations in matter and solar neutrino spectroscopy. *Nuovo Cim. C*, 9:17–26, 1986.

[50] P. F. De Salas, S. Gariazzo, O. Mena, C. A. Ternes, and M. Tórtola. Neutrino Mass Ordering from Oscillations and Beyond: 2018 Status and Future Prospects. *Front. Astron. Space Sci.*, 5:36, 2018.

PoS(CORFU2021)321

[51] B. T. Cleveland, Timothy Daily, Raymond Davis, Jr., James R. Distel, Kenneth Lande, C. K. Lee, Paul S. Wildenhain, and Jack Ullman. Measurement of the solar electron neutrino flux with the Homestake chlorine detector. *Astrophys. J.*, 496:505–526, 1998.

[52] F. Kaether, W. Hampel, G. Heusser, J. Kiko, and T. Kirsten. Reanalysis of the GALLEX solar neutrino flux and source experiments. *Phys. Lett. B*, 685:47–54, 2010.

[53] J. N. Abdurashitov et al. Measurement of the solar neutrino capture rate with gallium metal. III: Results for the 2002–2007 data-taking period. *Phys. Rev. C*, 80:015807, 2009.

[54] G. Bellini et al. Final results of Borexino Phase-I on low energy solar neutrino spectroscopy. *Phys. Rev. D*, 89(11):112007, 2014.

[55] G. Bellini et al. Precision measurement of the 7Be solar neutrino interaction rate in Borexino. *Phys. Rev. Lett.*, 107:141302, 2011.

[56] B. Aharmim et al. Combined Analysis of all Three Phases of Solar Neutrino Data from the Sudbury Neutrino Observatory. *Phys. Rev. C*, 88:025501, 2013.

[57] J. Hosaka et al. Solar neutrino measurements in super-Kamiokande-I. *Phys. Rev. D*, 73:112001, 2006.

[58] J. P. Cravens et al. Solar neutrino measurements in Super-Kamiokande-II. *Phys. Rev. D*, 78:032002, 2008.

[59] K. Abe et al. Solar neutrino results in Super-Kamiokande-III. *Phys. Rev. D*, 83:052010, 2011.

[60] Y. Nakano. PhD Thesis, University of Tokyo. http://www-sk.icrr.u-tokyo.ac.jp/sk/_pdf/articles/2016/doc_thesis_naknao.pdf, 2016.

[61] A. Gando et al. Constraints on θ_{13} from A Three-Flavor Oscillation Analysis of Reactor Antineutrinos at KamLAND. *Phys. Rev. D*, 83:052002, 2011.

[62] Y. Abe et al. Improved measurements of the neutrino mixing angle θ_{13} with the Double Chooz detector. *JHEP*, 10:086, 2014. [Erratum: JHEP 02, 074 (2015)].

[63] Y. Abe et al. Measurement of θ_{13} in Double Chooz using neutron captures on hydrogen with novel background rejection techniques. *JHEP*, 01:163, 2016.

[64] G. Bak et al. Measurement of Reactor Antineutrino Oscillation Amplitude and Frequency at RENO. *Phys. Rev. Lett.*, 121(20):201801, 2018.

[65] Jonghee Yoo. Reno, June 2020.

[66] D. Adey et al. Measurement of the Electron Antineutrino Oscillation with 1958 Days of Operation at Daya Bay. *Phys. Rev. Lett.*, 121(24):241805, 2018.

[67] K. Abe et al. Atmospheric neutrino oscillation analysis with external constraints in Super-Kamiokande I-IV. *Phys. Rev. D*, 97(7):072001, 2018.

PoS(CORFU2021)321

[68] Super-kamiokande atmospheric oscillation analysis 2020 (preliminary) results.

[69] M. G. Aartsen et al. Measurement of Atmospheric Neutrino Oscillations at 6–56 GeV with IceCube DeepCore. *Phys. Rev. Lett.*, 120(7):071801, 2018.

[70] M. G. Aartsen et al. Measurement of Atmospheric Tau Neutrino Appearance with IceCube DeepCore. *Phys. Rev. D*, 99(3):032007, 2019.

[71] A. Albert et al. Measuring the atmospheric neutrino oscillation parameters and constraining the 3+1 neutrino model with ten years of ANTARES data. *JHEP*, 06:113, 2019.

[72] Lodewijk Nauta et al. First neutrino oscillation measurement in KM3NeT/ORCA. *PoS*, ICRC2021:1123, 2021.

[73] M. H. Ahn et al. Measurement of Neutrino Oscillation by the K2K Experiment. *Phys. Rev. D*, 74:072003, 2006.

[74] P. Adamson et al. Combined analysis of ν_μ disappearance and $\nu_\mu \to \nu_e$ appearance in MINOS using accelerator and atmospheric neutrinos. *Phys. Rev. Lett.*, 112:191801, 2014.

[75] Patrick Dunne. Latest Neutrino Oscillation Results from T2K, jul 2020.

[76] Alex Himmel. New Oscillation Results from the NOvA Experiment, jul 2020.

[77] Núria Vinyoles, Aldo M. Serenelli, Francesco L. Villante, Sarbani Basu, Johannes Bergström, M. C. Gonzalez-Garcia, Michele Maltoni, Carlos Peña Garay, and Ningqiang Song. A new Generation of Standard Solar Models. *Astrophys. J.*, 835(2):202, 2017.

[78] John N. Bahcall and Roger K. Ulrich. Solar Models, Neutrino Experiments and Helioseismology. *Rev. Mod. Phys.*, 60:297–372, 1988.

[79] John N. Bahcall. The Be-7 solar neutrino line: A Reflection of the central temperature distribution of the sun. *Phys. Rev. D*, 49:3923–3945, 1994.

[80] John N. Bahcall, E. Lisi, D. E. Alburger, L. De Braeckeleer, S. J. Freedman, and J. Napolitano. Standard neutrino spectrum from B-8 decay. *Phys. Rev. C*, 54:411–422, 1996.

[81] John N. Bahcall. Gallium solar neutrino experiments: Absorption cross-sections, neutrino spectra, and predicted event rates. *Phys. Rev. C*, 56:3391–3409, 1997.

[82] B. Aharmim et al. An Independent Measurement of the Total Active B-8 Solar Neutrino Flux Using an Array of He-3 Proportional Counters at the Sudbury Neutrino Observatory. *Phys. Rev. Lett.*, 101:111301, 2008.

[83] Gabriela Barenboim, Christoph Andreas Ternes, and Mariam Tórtola. Neutrinos, DUNE and the world best bound on CPT invariance. *Phys. Lett. B*, 780:631–637, 2018.

[84] Maria Amparo Tórtola, Gabriela Barenboim, and Christoph Andreas Ternes. CPT and CP, an entangled couple. *JHEP*, 07:155, 2020.

PoS(CORFU2021)321

[85] T. Araki et al. Measurement of neutrino oscillation with KamLAND: Evidence of spectral distortion. *Phys. Rev. Lett.*, 94:081801, 2005.

[86] S. Abe et al. Precision Measurement of Neutrino Oscillation Parameters with KamLAND. *Phys. Rev. Lett.*, 100:221803, 2008.

[87] P. F. de Salas, D. V. Forero, S. Gariazzo, P. Martínez-Miravé, O. Mena, C. A. Ternes, M. Tórtola, and J. W. F. Valle. 2020 global reassessment of the neutrino oscillation picture. *JHEP*, 02:071, 2021.

[88] Y. Ashie et al. Evidence for an oscillatory signature in atmospheric neutrino oscillation. *Phys. Rev. Lett.*, 93:101801, 2004.

[89] M. Apollonio et al. Search for neutrino oscillations on a long baseline at the CHOOZ nuclear power station. *Eur. Phys. J. C*, 27:331–374, 2003.

[90] Francesco Capozzi, Eleonora Di Valentino, Eligio Lisi, Antonio Marrone, Alessandro Melchiorri, and Antonio Palazzo. Unfinished fabric of the three neutrino paradigm. *Phys. Rev. D*, 104(8):083031, 2021.

[91] Ivan Esteban, M. C. Gonzalez-Garcia, Michele Maltoni, Thomas Schwetz, and Albert Zhou. The fate of hints: updated global analysis of three-flavor neutrino oscillations. *JHEP*, 09:178, 2020.

[92] A. Aguilar-Arevalo et al. Evidence for neutrino oscillations from the observation of $\bar{\nu}_e$ appearance in a $\bar{\nu}_\mu$ beam. *Phys. Rev. D*, 64:112007, 2001.

[93] A. A. Aguilar-Arevalo et al. Updated MiniBooNE neutrino oscillation results with increased data and new background studies. *Phys. Rev. D*, 103(5):052002, 2021.

[94] G. Mention, M. Fechner, Th. Lasserre, Th. A. Mueller, D. Lhuillier, M. Cribier, and A. Letourneau. The Reactor Antineutrino Anomaly. *Phys. Rev. D*, 83:073006, 2011.

[95] C. Giunti, Y. F. Li, C. A. Ternes, and Z. Xin. Reactor antineutrino anomaly in light of recent flux model refinements. 10 2021.

[96] J. N. Abdurashitov et al. Measurement of the response of the Russian-American gallium experiment to neutrinos from a Cr-51 source. *Phys. Rev. C*, 59:2246–2263, 1999.

[97] J. N. Abdurashitov et al. Measurement of the response of a Ga solar neutrino experiment to neutrinos from an Ar-37 source. *Phys. Rev. C*, 73:045805, 2006.

[98] V. V. Barinov et al. Results from the Baksan Experiment on Sterile Transitions (BEST). 9 2021.

[99] P. Adamson et al. Search for Sterile Neutrinos Mixing with Muon Neutrinos in MINOS. *Phys. Rev. Lett.*, 117(15):151803, 2016.

PoS(CORFU2021)321

[100] P. Adamson et al. Search for sterile neutrinos in MINOS and MINOS+ using a two-detector fit. *Phys. Rev. Lett.*, 122(9):091803, 2019.

[101] M. G. Aartsen et al. Search for sterile neutrino mixing using three years of IceCube DeepCore data. *Phys. Rev. D*, 95(11):112002, 2017.

[102] M. G. Aartsen et al. eV-Scale Sterile Neutrino Search Using Eight Years of Atmospheric Muon Neutrino Data from the IceCube Neutrino Observatory. *Phys. Rev. Lett.*, 125(14):141801, 2020.

[103] S. Gariazzo, C. Giunti, M. Laveder, and Y. F. Li. Updated Global 3+1 Analysis of Short-BaseLine Neutrino Oscillations. *JHEP*, 06:135, 2017.

[104] Mona Dentler, Álvaro Hernández-Cabezudo, Joachim Kopp, Pedro A. N. Machado, Michele Maltoni, Ivan Martinez-Soler, and Thomas Schwetz. Updated Global Analysis of Neutrino Oscillations in the Presence of eV-Scale Sterile Neutrinos. *JHEP*, 08:010, 2018.

[105] S. Gariazzo, P. F. de Salas, and S. Pastor. Thermalisation of sterile neutrinos in the early Universe in the 3+1 scheme with full mixing matrix. *JCAP*, 07:014, 2019.

[106] N. Aghanim et al. Planck 2018 results. VI. Cosmological parameters. *Astron. Astrophys.*, 641:A6, 2020. [Erratum: Astron.Astrophys. 652, C4 (2021)].

[107] O. G. Miranda, M. A. Tortola, and J. W. F. Valle. Are solar neutrino oscillations robust? *JHEP*, 10:008, 2006.

[108] André de Gouvêa and Kevin J. Kelly. Non-standard Neutrino Interactions at DUNE. *Nucl. Phys. B*, 908:318–335, 2016.

[109] Y. Farzan and M. Tortola. Neutrino oscillations and Non-Standard Interactions. *Front. in Phys.*, 6:10, 2018.

[110] F. J. Escrihuela, D. V. Forero, O. G. Miranda, M. Tortola, and J. W. F. Valle. On the description of nonunitary neutrino mixing. *Phys. Rev. D*, 92(5):053009, 2015. [Erratum: Phys.Rev.D 93, 119905 (2016)].

[111] O. G. Miranda, M. Tortola, and J. W. F. Valle. New ambiguity in probing CP violation in neutrino oscillations. *Phys. Rev. Lett.*, 117(6):061804, 2016.

[112] Don Colladay and V. Alan Kostelecky. CPT violation and the standard model. *Phys. Rev. D*, 55:6760–6774, 1997.

[113] Don Colladay and V. Alan Kostelecky. Lorentz violating extension of the standard model. *Phys. Rev. D*, 58:116002, 1998.

[114] V. Alan Kostelecky. Gravity, Lorentz violation, and the standard model. *Phys. Rev. D*, 69:105009, 2004.

PoS(CORFU2021)321

[115] V. Alan Kostelecky and Matthew Mewes. Lorentz and CPT violation in neutrinos. *Phys. Rev. D*, 69:016005, 2004.

[116] Alan Kostelecky and Matthew Mewes. Neutrinos with Lorentz-violating operators of arbitrary dimension. *Phys. Rev. D*, 85:096005, 2012.

[117] P. Adamson et al. Search for Lorentz invariance and CPT violation with muon antineutrinos in the MINOS Near Detector. *Phys. Rev. D*, 85:031101, 2012.

[118] M. G. Aartsen et al. Neutrino Interferometry for High-Precision Tests of Lorentz Symmetry with IceCube. *Nature Phys.*, 14(9):961–966, 2018.

[119] B. Aharmim et al. Tests of Lorentz invariance at the Sudbury Neutrino Observatory. *Phys. Rev. D*, 98(11):112013, 2018.

[120] Gabriela Barenboim, Mehedi Masud, Christoph A. Ternes, and Mariam Tórtola. Exploring the intrinsic Lorentz-violating parameters at DUNE. *Phys. Lett. B*, 788:308–315, 2019.

[121] K. Abe et al. Updated T2K measurements of muon neutrino and antineutrino disappearance using 1.5×10^{21} protons on target. *Phys. Rev. D*, 96(1):011102, 2017.

PoS(CORFU2021)321